

AD-752 228

OAO, A-2 (ORBITING ASTRONOMICAL OBSERVATORY
A-2) MEASUREMENTS OF THE ULTRAVIOLET AIR-
GLOW

Edward S. Fishburne, et al

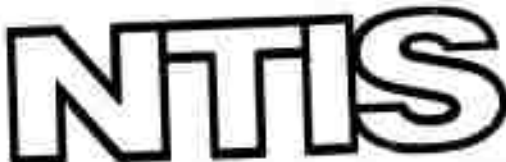
Grumman Aerospace Corporation

Prepared for:

Air Force Cambridge Research Laboratories
Advanced Research Projects Agency

30 September 1972

DISTRIBUTED BY:



National Technical Information Service
U. S. DEPARTMENT OF COMMERCE
5285 Port Royal Road, Springfield Va. 22151

**BEST
AVAILABLE COPY**

AFCRL-72-0318

OAO, A-2, MEASUREMENTS
OF THE ULTRAVIOLET AIRGLOW

by

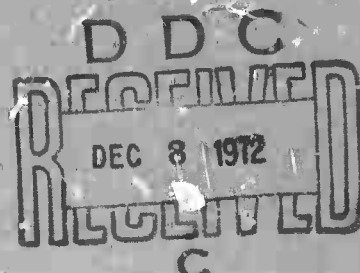
Edward S. Fishburne Charles R. Waters
Donald L. Moyer Barnett S. Green

Grumman Aerospace Corporation
Bethpage, New York 11714

Contract No. F19628-71-C-0129
Project No. 8692

FINAL REPORT
March 1971 - September 1972

30 September 1972



Contract Monitor: Arthur K. Holmes
Optical Physics Laboratory

Reproduced by
NATIONAL TECHNICAL
INFORMATION SERVICE
U.S. Department of Commerce
Springfield VA 22151

Approved for Public Release; Distribution Unlimited

Sponsored by
DEFENSE ADVANCED RESEARCH PROJECTS AGENCY
ARPA Order No. 1366

Monitored by
AIR FORCE CAMBRIDGE RESEARCH LABORATORIES
AIR FORCE SYSTEMS COMMAND
UNITED STATES AIR FORCE
BEDFORD, MASSACHUSETTS 01730

Details of illustrations in
this document may be better
studied on microfiche

ARPA Order No.: 1366
Program Code No.: 1E50
Name of Contractor: Grumman Aerospace Corporation
Effective Date of Contract: 1 February 1971

Contract No.: F19628-71-C-0129
Principal Investigator and Phone No.: Dr. Edward S. Fishburne
(516) 575-2229
AFCRL Project Scientist and Phone No.: Arthur K. Holmes
(616) 861-2952
Contract Expiration Date: 30 April 1972



Qualified requesters may obtain additional copies from the Defense Documentation Center. All others should apply to the National Technical Information Service.

DOCUMENT CONTROL DATA - R&D

(Security classification of title, body of abstract and indexing annotation must be entered when the overall report is classified)

1. ORIGINATING ACTIVITY (Corporate author) Grumman Aerospace Corporation Bethpage, New York 11714		2a. REPORT SECURITY CLASSIFICATION Unclassified
		2b. GROUP

3. REPORT TITLE

OAO, A-2, MEASUREMENTS OF THE ULTRAVIOLET AIRGLOW

4. DESCRIPTIVE NOTES (Type of report and inclusive dates) Scientific Final March 1971-September 1972			Approved: 25 Sept. 1972
---	--	--	----------------------------

5. AUTHOR(S) (First name, middle initial, last name) Edward S. Fishburne Donald L. Moyer		Charles R. Waters Barnett S. Green	
--	--	---------------------------------------	--

6. REPORT DATE 30 September 1972	7a. TOTAL NO. OF PAGES 71	7b. NO. OF REFS 21
-------------------------------------	------------------------------	-----------------------

8a. CONTRACT OR GRANT NO. F19628-71-C-0129	9a. ORIGINATOR'S REPORT NUMBER(S)
---	-----------------------------------

b. PROJECT, TASK, WORK UNIT NOS. 8629 n/a n/a	9b. OTHER REPORT NO(S) (Any other numbers that may be assigned this report)
--	---

c. DOD ELEMENT 62301D	AFCRL-72-0318
--------------------------	---------------

d. DOD SUBELEMENT n/a	
--------------------------	--

10. DISTRIBUTION STATEMENT Approved for Public Release; distribution unlimited.	
--	--

11. SUPPLEMENTARY NOTES Details of illustrations in this document may be better studied on microfiche	12. SPONSORING MILITARY ACTIVITY Air Force Cambridge Research Laboratory (OP) L.G. Hanscom Field Bedford, Massachusetts 01730
--	--

13. ABSTRACT The term airglow is commonly used to describe nonthermal emissions not correlated with magnetic disturbances in the upper atmosphere. The study of this radiation provides information on the nature of the upper atmosphere, as well as clues to the physical processes occurring at very high altitudes. The spectral region below 3000 Å is one of the most informative wavelength intervals, but the opacity of the atmosphere in this part of the spectrum prevents adequate measurement of ultraviolet emissions except by rockets and satellites. To obtain more information, we undertook an investigation to measure the dark and sunlit earth using the Wisconsin Experiment Package (WEP) photometers of the Orbiting Astronomical Observatory A-2. The first series of measurements were concerned with the magnitude of the emitted radiation. Based on findings indicated by these measurements, we began concentrating on measurements of the earth limb. We used the 2980, 2460, 2380, 1920, 1500, 1380, and 1250Å filters of the WEP stellar photometers. Our experimental results tend support the theory that dayglow in the 1300-1800Å region is due primarily to photoelectron excitation of molecular nitrogen. The measurements obtained on the earth's limb represent the most complete coverage known to the authors.	
--	--

Unclassified

Security Classification

14. KEY WORDS	LINK A		LINK B		LINK C	
	ROLE	WT	HOLE	WT	ROLE	WT
Airglow Earth Limb Nonthermal emissions Ultraviolet Atmosphere Radiation						

iB

Unclassified

Security Classification

OAO, A-2, MEASUREMENTS
OF THE ULTRAVIOLET AIRGLOW

by

Edward S. Fishburne Charles R. Waters
Donald L. Moyer Barnett S. Green

Grumman Aerospace Corporation
Bethpage, New York 11714

Contract No. F19628-71-C-0129
Project No. 8692

FINAL REPORT
March 1971 - September 1972

30 September 1972

Contract Monitor: Arthur K. Holmes
Optical Physics Laboratory

Approved for Public Release; Distribution Unlimited

Sponsored by
DEFENSE ADVANCED RESEARCH PROJECTS AGENCY
ARPA Order No. 1366

Monitored by
AIR FORCE CAMBRIDGE RESEARCH LABORATORIES
AIR FORCE SYSTEMS COMMAND
UNITED STATES AIR FORCE
BEDFORD, MASSACHUSETTS 01730

IC

ABSTRACT

The term airglow is commonly used to describe nonthermal emissions not correlated with magnetic disturbances in the upper atmosphere. The study of this radiation provides information on the nature of the upper atmosphere, as well as clues to the physical processes occurring at very high altitudes. The spectral region below 3000\AA is one of the most informative wavelength intervals, but the opacity of the atmosphere in this part of the spectrum prevents adequate measurement of ultraviolet emissions except by rocket and satellite. Until recently, most measurements were restricted to rocket flights at high altitudes, although a limited amount of information was obtained by several satellites in the OGO series, in particular, OGO-4 (Refs. 1-5).

To obtain more information about the earth's ultraviolet airglow, we undertook an investigation to measure the dark and sunlit earth using the Wisconsin Experiment Package (WEP) photometers of the Orbiting Astronomical Observatory A-2. The first series of measurements were concerned with the magnitude of the emitted radiation. Based on findings indicated by these measurements, we began concentrating on measurements of the earth limb. The small field of view of the WEP package has a fine spatial resolution, providing a detailed picture of the ultraviolet radiation in the earth's limb. Our measurements used the 2980, 2460, 2380, 1920, 1500, 1380, and 1250\AA filters of the WEP stellar photometers.

The measurements obtained on the earth's limb represent the most complete coverage known to the authors. In addition, measurements in selected spectral regions provide the first information available on these regions and confirm observations by previous investigators. Finally, our experimental results tend to substantiate the theory that the dayglow in the $1300\text{-}1800\text{\AA}$ region is primarily due to photoelectron excitation of molecular nitrogen.

TABLE OF CONTENTS

<u>Item</u>	<u>Page</u>
Introduction	1
The Orbiting Astronomical Observatory A-2	8
Data Reduction	15
Data Analysis	37
Summary and Conclusions	59
References	61

LIST OF ILLUSTRATIONS

<u>Figure</u>		<u>Page</u>
1	Various Experimental Measurements of the Earth's Radiance and the Theoretical Values Based on Rayleigh Scattering	6
2	Relative Response of WEP Filters	9
3	Relative Position of Earth and OAO during Typical Measurement Sequence	12
4	Ground Track of OAO Field of View during Measurement Sequence Depicted in Fig. 3	14
5	Received Radiation Measured with 1250Å Filter	16
6	Received Radiation Measured with 1920Å Filter	17
7	Received Radiation Measured with 1500Å Filter	18
8	Typical Viewing Geometry	20
9	Variation of Angles for Orbit 7903	45
10	Comparison of OAO Measurements with Other Experimental Measurements. Values are for 1380Å, 1500Å, and 1920Å Filters. Lower line represents the measured value minus the expected contribution of the 1304Å oxygen line.	46
11	1500Å Limb Measurement	48
12	Altitude Profile of 1500Å Radiation	49
13	Altitude Profile of 1500Å Radiation	50
14	Altitude Profile of 1500Å Radiation	51
15	Altitude Profile of 1920Å Radiation	52
16	Altitude Profile of 1250Å Radiation	53

<u>Figure</u>		<u>Page</u>
17	Altitude Profile of the 1920 \AA Nightglow	55
18	Altitude Profile of the 2980 \AA Nightglow	56
19	Altitude Profile of 2380 \AA Nightglow	57
20	Altitude Profile of the 2460 \AA Nightglow	58

INTRODUCTION

Airglow and auroras have been subjects of considerable research during the past century. The most comprehensive analysis is that given by Chamberlain (Ref. 6), which contains more than 1600 references, compiled through 1959, to the literature. Most of these references concern ground observations of the visible airglow. Due to atmospheric absorption, however, measurements of ultraviolet emissions of the upper atmosphere have been limited to rocket and satellite observations. Tables 1-3 summarize the important ultraviolet experiments flown since 1963.

The most important features of the earth's airglow below 2000\AA are the Lyman alpha emissions of atomic hydrogen at 1216\AA and the emissions from the 1302 , 1305 , and 1306\AA triplet of atomic oxygen. The Lyman alpha emission is produced by the resonance scattering of the Sun's Lyman alpha line, the strongest emission line in the solar spectrum. Most of the early rocket measurements (Ref. 7) concentrated on this particular feature. A long term study of the Lyman alpha corona was made by the Naval Research Laboratory Experiment, using OGO-4 (Ref. 4). From these measurements, Meier developed a detailed description and theory of the Lyman alpha geo-corona. The atomic oxygen lines, including the 1356\AA line, have been studied thoroughly in the past few years (Refs. 8-10). It appears that these emissions of atomic oxygen are produced by photoelectron excitation. This mechanism also appears to produce the weaker emissions from atomic nitrogen at 1200 , 1493 , and 1744\AA .

Barth (Ref. 2) has shown that the dominant radiation between 1358 and 1700\AA is that due to the Lyman-Birge-Hopfield, the Birge-Hopfield, and the Vergard-Kaplin bands of molecular nitrogen. Theoretical investigations by Barth and by Green (Ref. 9) indicate that the emissions from these bands appear to be produced also by photoelectron excitation. The other major feature of the ultraviolet dayglow is the gamma bands of nitric oxide that are observed in resonance fluorescence (Ref. 11).

Measurements of the earth's dayglow (between 1700 and 3000\AA) agree very well with calculations based on Rayleigh scattering, including absorption by ozone and absorption by molecular oxygen. We have indicated in Fig. 1 our calculation of the earth dayglow, which would result from first order Rayleigh scattering for a spherical atmosphere in the region between 1000 and 2000\AA . The actual magnitude of the earth's dayglow will depend on the values

Table 1

OBSERVATIONS OF THE ULTRAVIOLET DAYGLOW

Reference	Wavelength Region	Quoted Measurement	Earth Radiance $\text{W/cm}^2 \cdot \text{Ster} \cdot \text{u}$	Comments
Friedman, Rawcliffe & Meloy - 1963	2450 - 2850 Å	$2 \times 10^{-5} \text{ W/cm}^2 \cdot \text{Ster} \cdot \text{u}$	$\approx 10^{-5}$	Satellite measurement Radiometer with $\lambda_c = 2550 \text{ Å}$, polar angle = 49° . FOV = $1.2 \times 10^{-4} \text{ Ster} = .7^\circ$ Sens. = $5 \times 10^{-6} \text{ W/cm}^2 \cdot \text{Ster} \cdot \text{u}$
Hinesee, Fastie & Jankiewicz - 1964	2000 - 2700 Å	(.4-2) erg/sec-cm ² -ster -100 Å	(.1-2) $\times 10^{-4}$	Rocket flight Photometer $\lambda_c = 2200 \text{ Å}$ $\Delta\lambda = 230 \text{ Å}$ $\lambda_c = 2600 \text{ Å}$ $\Delta\lambda = 1.0 \text{ Å}$ Solar angle = 22°
Barth - 1964	1500-3500 Å	2 KR at 2155 Å	1.47×10^{-7}	Aerobee - spectrometer Altitude = 75° - 116 Km Sun angle = 60° Resolution = 10 \AA 3 bands of 30 most prominent feature - Produced by instrument drift.
Pastie Crosswhite & Heath - 1964	1216 Å 1304 Å 1356 Å	13 Kr 7 Kr .4 Kr	100×10^{-6} 5.03×10^{-7} $\approx 7.6 \times 10^{-8}$	Aerobee Altitude = 210 km max. Resolution = 17 \AA Peak in 1304 at 190 km Peak in 1356 at 135 km
Rawcliffe & Elliott - 1966	2000 - 3200 Å	(.2 - 2.5) $\times 10^{-10} \text{ W/cm}^2 \cdot \text{ster-A}$	(.2 - 9.5) $\times 10^{-6}$	Rocket observation Sun elevation = -14° Twilight condition
Moos & Pastie - 1967	1216 Å 1304	3.6 Kr at 152 km 110 R	3.14×10^{-7} 3.95×10^{-9}	Rocket observation Altitude = 60-95 km Twilight condition Sun zenith = 92° Resolution = 12 \AA (1,0) band or NO Mott gradient
Pearce - 1969	2070 - 2370 Å	2155 Å 10 KR at 60 km 1 KR at 95 km	6.15×10^{-7} 6.15×10^{-8}	Rocket observation Altitude = 60-95 km Twilight condition Sun zenith = 92° Resolution = 12 \AA (1,0) band or NO Mott gradient

Table 1
OBSERVATIONS OF THE ULTRAVIOLET DAYLIGT - (Continued)

Reference	Wavelength Region	Quoted Measurement	Particulate Emissance %	Comments
Barth & Mackey 1969	1150 - 3350 Å	1216 Å = 30 KR/20 Å 1304 Å = 20 KR/20 Å 1356 Å = 2 KR/20 Å 2550 Å = 30 KR/20 Å	1.95 x 10 ⁻⁶ 1.25 x 10 ⁻⁶ 1.17 x 10 ⁻⁷ 9.35 x 10 ⁻⁷	OGO IV - Spectrometer Sun zenith = 0° Resolution = 20 Å
Chubb & Hicks 1970	1050 - 1350 Å 1350 - 1550 Å	1216 Å = 26 KR 1304 Å = 15 KR 2.5 KR	2.27 x 10 ⁻⁶ 1.22 x 10 ⁻⁶ 1.37 x 10 ⁻⁸	OGO IV - No protoionization Chamber FOV = 65° 40'
Barth & Schaffner 1970	1150 - 3350 Å	1304 Å = 36.2 KR 1356 Å = 2 KR 1384 Å = 1.2 KR	2.21 x 10 ⁻⁶ 1.17 x 10 ⁻⁷ 6.90 x 10 ⁻⁸	OGO IV - Spectrometer Resolution = 20 Å Sun zenith = 31°

- 3 -

Reference	Wavelength Region	Quoted Measurement	Earth Radiance W/m ² - Ster - u	Comments
Stecker 1965	1500 - 3500	20-100 R/ \AA	(1.2 ⁻ - 5.3) $\times 10^{-5}$	Aerobee 4 spectrometer Resolution = 50 \AA Max. radiation received at 92.7 km at 3000 \AA through horizon.
Hemes	2300 - 3800	Avg. = .75 R/ \AA	3.37E $\times 10^{-7}$	Rocket observation spectrometer = 12 \AA Res. FOV = 2° Altitude = 184 km Zenith measurement Radiation due to Herzberg bands of O ₂
Winter & Chubb	1216 \AA	(1.1 - 10) $\times 10^{-3}$ ery/cm ² -sec-ster	(1.1 - 10) $\times 10^{-6}$	
Chubb & Hicks 1970	1050 - 1350 \AA	1.2 KR	5.3 $\times 10^{-9}$	OGO IV - NO photoionization Chubb Zenith Measurements FOV = (5° ^{40'})
Barth & Schaffner	1216 \AA 1304 \AA 1356 \AA	2.5 KR 1.7 KR 1.4 KR	1.64 $\times 10^{-7}$ 1.02 $\times 10^{-7}$ 5.22 $\times 10^{-8}$	OGO IV - Spectrometer Equatorial Nightglow Resolution = 20 \AA Zenith Measurements
Prinz & Meirer 1970	1304 \AA 1350 - 1600	4-6 KR 25 R	(3.254 ± .38) $\times 10^{-7}$ 1.1 $\times 10^{-10}$	OGO IV - NO photoionization Chubb Zenith Measurements

-X-

Table 3

OBSERVATIONS OF THE ULTRAVIOLET AURORA

Reference	Wavelength Region	Measurement	Earth Radiation	Comments
Teller & Faustle 1965	1452 + 2210	$\Delta V = 2.35 \text{ m}$	9.95×10^{-7} $\text{n/cm}^2 \cdot \text{ster} \cdot \text{sr}$	Rocket Observation and Spectrometer Resolution = 2 Å Sensitivity = 2.5 dB
Murphy	2000 + 1452 Å 2250 + 1350 Å	0.08×10^{-3} $\text{erg cm}^{-2} \text{ sec}^{-1} \text{ str}^{-1}$ $+ 0.2 \times 10^{-3}$	8×10^{-3} $- 8 \times 10^{-3}$	Zenith observation NO photopolarization Chamber POT = 1.0 g
Miller, Faustle & Teller 1973	1350 + 1350 Å 1220 + 1350 Å (NT) 1350 Å (GT) 1300	1.19 Å 15.4 Å 1.50 Å	1.06×10^{-7} 1.17×10^{-7} 2.77×10^{-7}	Short observation Photometer Altitude 20-30 km
Chubb & Hicks 1970	2000 1350 + 1350 Å 1350 + 1350 Å Slab	1.4 Å 2.57 Å 2.6 Å	1.34×10^{-7} 4.17×10^{-6}	GOO IV - NO Photoluminescence Chambers
	1050 + 1350 Å 1350 + 1350 Å	2.6 Å 1.0 Å	2.11×10^{-7} 7.3×10^{-8}	Zenith Measurements
Smith & Schaffner 1970	1306 Å 1356 Å 1356 Å (NT)	16.4 Å 3 Å 1.5 Å	9.89×10^{-7} 2.76×10^{-7} 6.05×10^{-8}	GOO IV - Spectrometer Zenith Measurements Resolution = 250

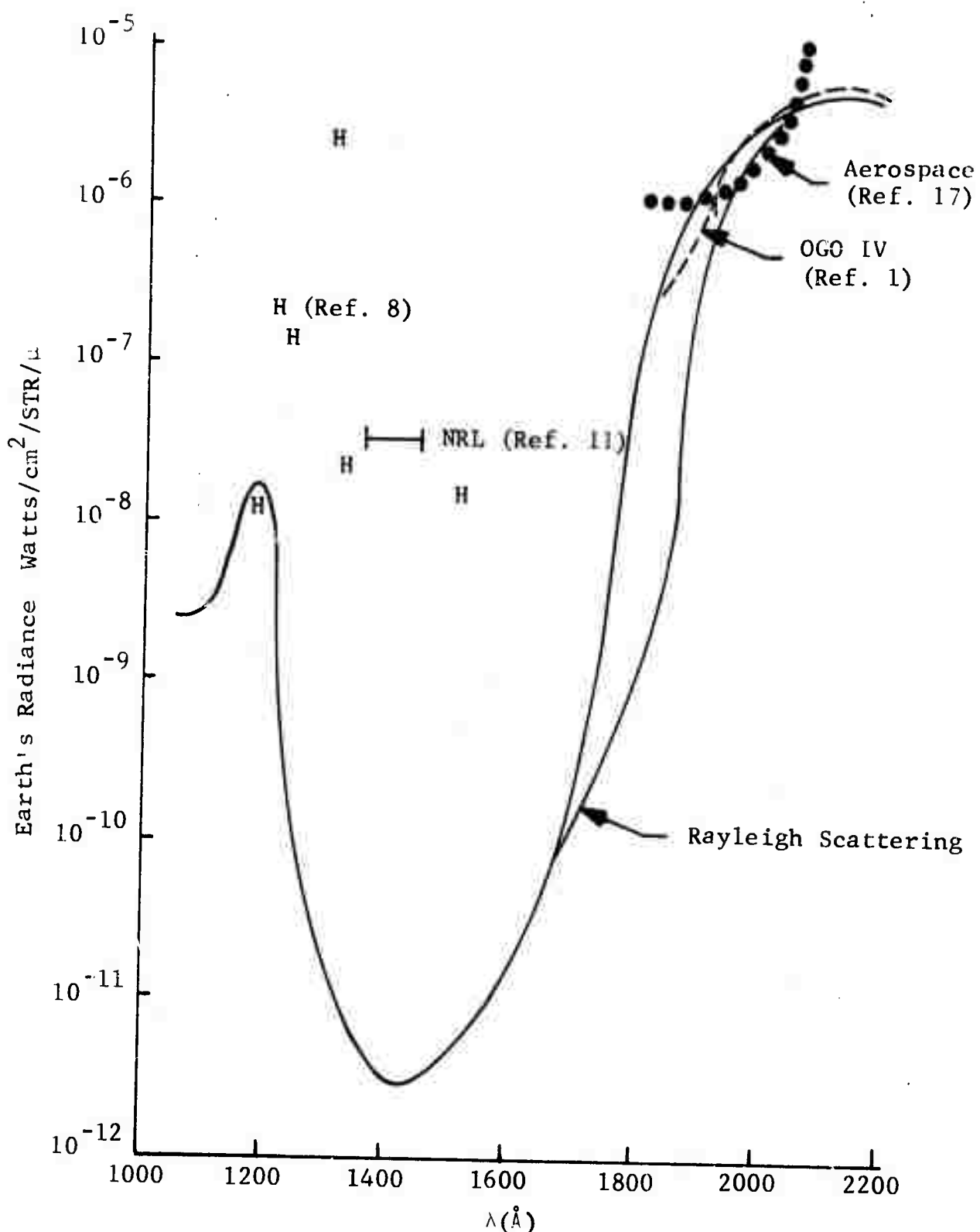


Fig. 1 Various Experimental Measurements of the Earth's Radiance and the Theoretical Values Based on Rayleigh Scattering

chosen for the absorption cross section of molecular oxygen. In addition, it is necessary that a molecular oxygen altitude profile be used in the calculation. For the calculation presented in Fig. 1, we used the ultraviolet flux from the sun as determined by Hinteregger (Ref. 12), the absorption coefficients from Ditchburn (Ref. 13), and the standard atmosphere for the molecular oxygen distribution. The selection of other values for the solar flux and the absorption coefficients or the choice of a different molecular oxygen distribution will tend to shift the curve slightly higher or slightly lower but not by a considerable amount.

The nightglow below 3000 \AA consists mainly of the Herzberg band of molecular oxygen that occurs primarily between 2500 and 3500 \AA (Refs. 14,15). The 2972 \AA line of atomic oxygen is also present. Below 2000 \AA , the only major radiation is that due to the Lyman alpha line (Refs. 2,7) and the 1304 \AA triplet of atomic oxygen (Refs. 3,5).

In a search of the literature for previous measurements of the earth's dayglow and nightglow, we have been unable to find any detailed spatial measurements of the earth's limb in the ultraviolet region below 3000 \AA . Some mention has been made of an apparent brightening effect, but no quantitative measurements were reported. Quantitative measurements are presented in this report.

THE ORBITING ASTRONOMICAL OBSERVATORY A-2

The NASA-Goddard/Grumman Orbiting Astronomical Observatory A-2 was launched 7 December 1968, its mission to make detailed ultraviolet measurements of stars, galaxies, and other heavenly bodies. A set of six-gimbal star trackers and a system of gyros enable the OAO to be pointed with an accuracy of 1 minute of arc and to hold a pointing ± 15 arc seconds once it has been stabilized. The A-2 is equipped with the Smithsonian Astrophysical Observatory (SAO) package and the Wisconsin Experiment Package (WEP). The SAO package is designed to make large field sky maps in the ultraviolet, and the WEP obtains precise photometric measurements of individual celestial objects.

The Wisconsin Experiment Package consists of seven instruments designed to make ultraviolet measurements of selected celestial objects. The package includes four 8-inch telescopes incorporating photoelectric photometers, two scanning objective grating spectrometers, and a 16-inch photometer that unfortunately failed after two months of operation.

Each 8-inch telescope has a five-position filter wheel that contains three different interference filters, dark slide, and calibration source. Each is an off-axis paraboloid with a focal length of 81 cm and an effective collecting area of 325 cm^2 . The two field stops available at the focal plane have angle diameters of 2 and 10 arc minutes. Stellar photometers 1 and 2 operate at above 1700\AA , while stellar photometers 3 and 4 cover the spectral region between 1200 and 2700\AA . The response curves for the given filter combinations utilized in the ultraviolet measurements reported in this investigation are shown in Fig. 2. Photometer 1, which contains the 2980\AA filter, employ EMR 6256B photomultipliers. Photometer 3, which contains the 2460 and 1920\AA filters, utilizes an EMR 541F photomultiplier, while Photometer 4, which has the 1250, 1380, and 1500\AA filters, employs an EMR 541G photomultiplier.

The photomultiplier signal is processed by a pulse counter and a d.c. amplifier, providing a digital and analog output, both of which are stored after each exposure. Exposure times of 1/8, 1, 8, or 64-second duration are available by command.

Several modes of operation are available to the experimenter, the choice depending on the type of investigation being conducted. The mode used for most of the airglow measurements was one in which the data sampling was controlled by the scanning spectrometers.

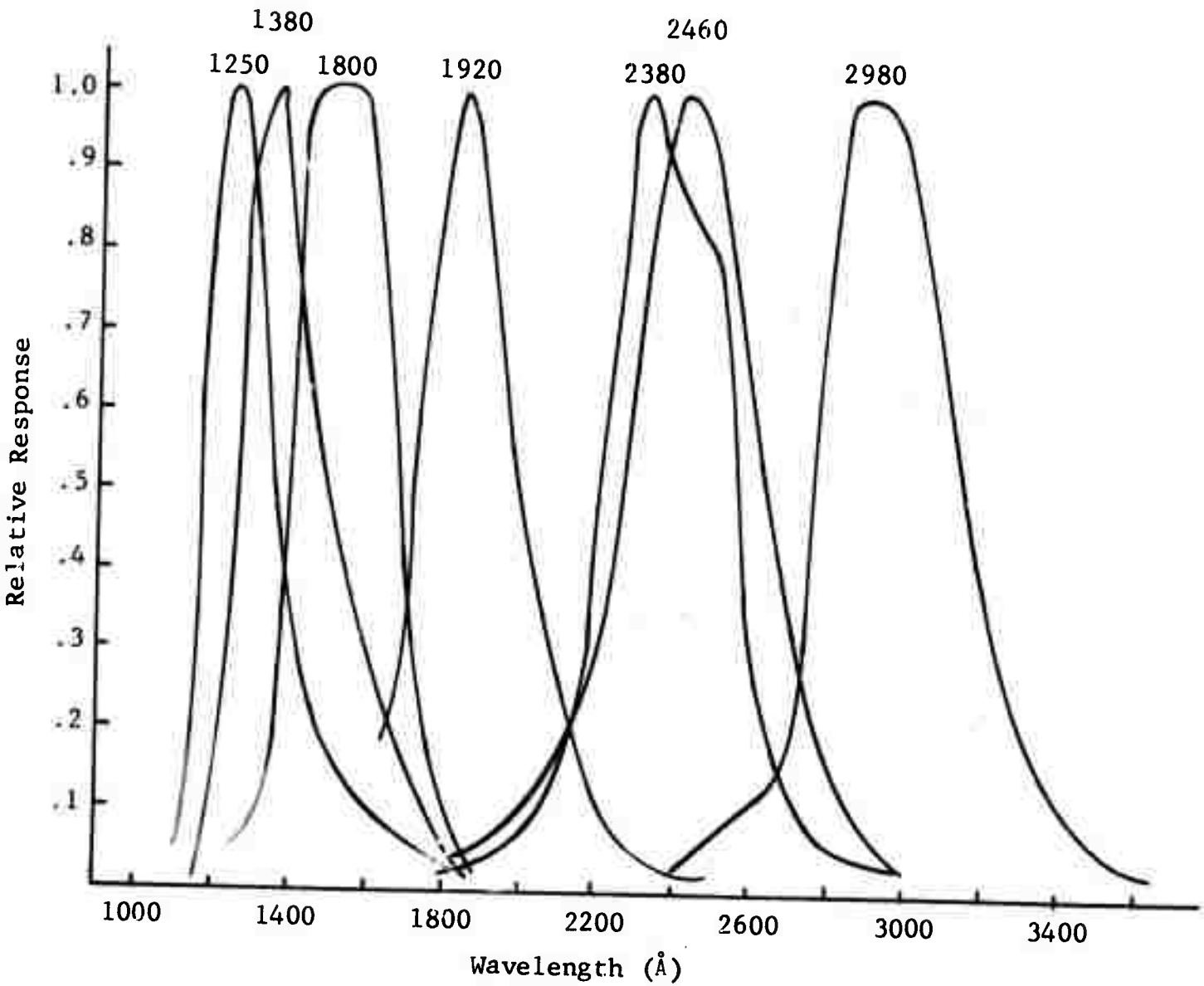


Fig. 2 Relative Response of WEP Filters

Table 4

CALIBRATION FACTORSEQUIVALENT RADIANCE(ω/cm²-ster-μ-count)

Filter	1/8 Sec Exposure	1/2 Sec Exposure	1 Sec Exposure	8 Sec Exposure	64 Sec Exposure
1250Å	1.25×10^{-7}	3.14×10^{-8}	1.57×10^{-8}	1.96×10^{-9}	2.5×10^{-10}
1380Å	6.04×10^{-8}	1.5×10^{-8}	7.55×10^{-9}	9.40×10^{-10}	1.2×10^{-10}
1500Å	2.89×10^{-8}	7.24×10^{-9}	3.63×10^{-9}	4.5×10^{-10}	5.82×10^{-11}
1920Å	7.73×10^{-10}	1.94×10^{-10}	9.71×10^{-11}	1.22×10^{-11}	1.56×10^{-12}
2380Å	4.03×10^{-10}	1.02×10^{-10}	5.07×10^{-11}	6.32×10^{-12}	7.94×10^{-13}
2460Å	2.96×10^{-10}	7.42×10^{-11}	3.70×10^{-11}	4.63×10^{-12}	5.79×10^{-13}
2980Å	7.4×10^{-11}	1.87×10^{-11}	9.46×10^{-12}	1.16×10^{-12}	1.45×10^{-13}

DEGRADATION FACTOR FOR PHOTOMETER 4

(I_{actual} = k I_{measured})

Filter \ Time	D 161-165 1970	D 268 1970	D 83 1971	D 148 1971	D 215 1971	D 225 1971
1250Å	1.58	2.51	8.32	9.12	10.0	10.0
1380Å	1.15	1.45	4.37	5.25	5.75	5.75
1500Å	1.10	1.20	1.58	1.74	2.09	2.09

- 9B -

One spectrometer was commanded to perform two consecutive 94-step scans. An 8-second exposure period exists between the completion of one step and the initiation of the next step. After the exposure, the data from all instruments are sampled. The actual time to perform a step is approximately 1 second. The exposure times of the photometers can be selected to be 1/8, 1, or 8 seconds and are initiated at the beginning of an 8-second spectrometer exposure.

Another mode of operation was employed for the detailed measurements of the earth's limb. In this mode, the exposure time for all instruments was set at 64 seconds. However, each instrument was sampled at 0.524 second intervals. A total of about $2\frac{1}{2}$ minutes of data can be stored in the spacecraft's data processing system using this mode. When the OAO is in real time contact with a ground station, this mode can provide up to 10 minutes of continuous data.

To obtain measurements of the earth's nightglow, we found it necessary to employ the 64-second exposure mode. This particular mode is the most sensitive, since the signals are integrated over the entire 64-second period. It cannot be used during daylight hours since the photometers would saturate.

The calibration factors for the various filters and modes of operation are given in Table 4. These factors were obtained from calibration tests made prior to launch. Other tests have been conducted in space to validate the factors.

To appreciate the data and the manner in which they were obtained, it is necessary that the reader fully understand the relation between the OAO line of sight (LOS) and the relative position of the earth. All observations were made by inertially fixing the OAO LOS in terms of right ascension and declination. This means that the OAO points at a particular spot on the celestial sphere. The OAO is inertially stabilized such that it will continue pointing at that spot until commanded to another position. Thus, we cannot command the OAO to look at a particular point on the surface of the earth and to follow that point since this was not the original intent of the OAO. Once the OAO is pointed at a particular spot on the celestial sphere, we can obtain measurements of the earth's dayglow, nightglow, and limb by exposing during the time the desired portion of the earth moves through the field of view of the OAO. The position of the OAO relative to the earth during a typical measurement sequence is depicted in Fig. 3. The three positions of the OAO shown in the illustration correspond

GEOMETRY OF OAO, ORBIT 7903

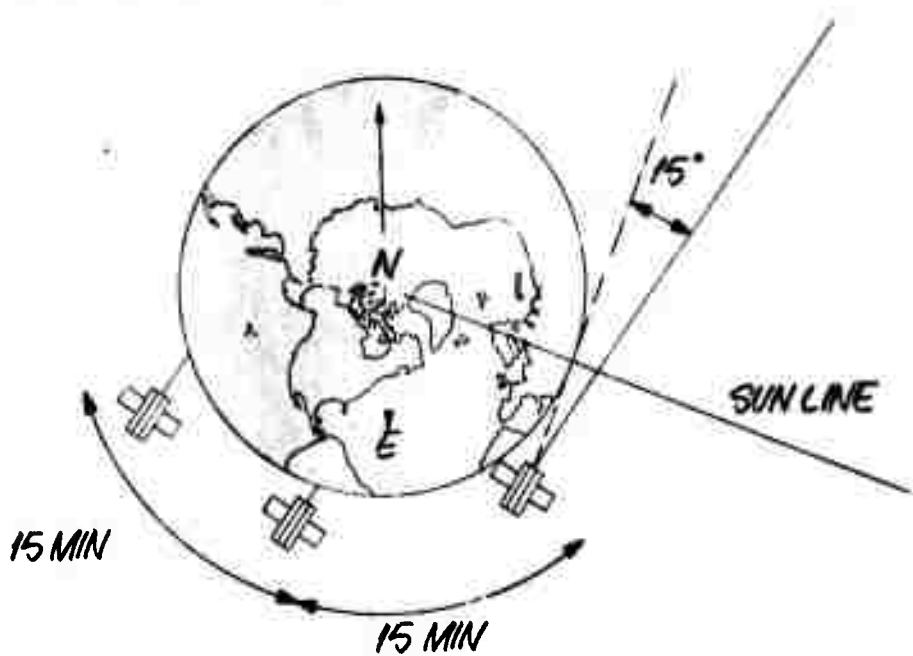
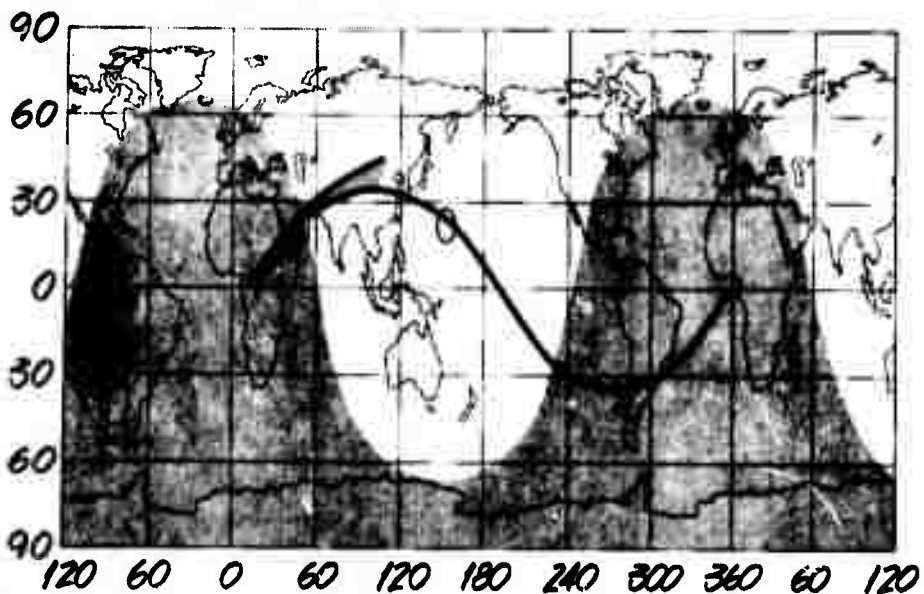


Fig. 3 Relative Position of Earth and OAO
during Typical Measurement Sequence

to the position at the beginning, middle, and end of a half-hour measurement sequence. Note in the illustration that the measurements were initially made of the dark earth, then the sunlit portion of the earth, and finally the sunlit limb. Also note that the total amount of sunlit atmosphere in the field of view increases as the earth moves through the field of view. Figure 4 indicates the ground track of the OAO field of view during the measurements period. The viewing situation is typical of those made during the first set of observations and characterizes the manner in which all measurements were made.

OAO MEASUREMENTS

• OAO ORBIT 7903: 10 JUNE 1970



Reproduced from
best available copy.

Fig. 4 Ground Track of OAO Field of View
during Measurement Sequence Depicted
in Fig. 3

DATA REDUCTION

Wisconsin Experiment Package measurements of the earth airglow were made at several different times during 1970-1971. The bulk of the measurements were made over a four-day period (June 10 through June 13, 1970) on 27 different orbits. This set of observations was obtained by programming the OAO to view a star, Alpha-Leo, and to expose during the time this star was occulted by the earth. Each measurement period was approximately 30 minutes long and consisted of a series of 188 exposures of either 1/8, 1, or 8 seconds duration. The experiment was operated in the mode in which the scanning spectrometer controlled the sampling period. Figure 4 indicates the ground track of orbit 7903 during the measurement period.

The variation of the received radiation as the viewing area scans across the earth is indicated in Figs. 5-7. The received radiation is given in terms of the original digital counts or voltage as transmitted from the OAO. Figures 5 and 6 represent data obtained during orbit 7903. Figure 5 indicates the radiation received by the 1250 \AA photometer and Fig. 6 represents that received by the 1920 \AA photometer. An interesting feature is apparent on examining these two curves: radiation in the 1250 \AA regions appears to reach a maximum value after the field of view has left the surface of the earth. This maximum occurs at a tangent altitude of about 175 kilometers. On the other hand, the 1920 \AA photometer indicates that as the field of view moves off the earth's surface, the radiation begins to decrease rapidly. Figure 7 depicts the radiation received by the 1500 \AA photometer during a later orbit. This radiation also peaks at a tangent altitude of about 175 kilometers.

The presence of the peak in the radiation indicates that the source of radiation in the 1200-1600 \AA region is different from that in the 1900 \AA region. The explanation and theoretical models for these two sources of radiation are given later. Also discussed in a later section is the method of reducing the data to some common basis such that comparisons to other experimental results can be made.

A considerable amount of data was obtained on the earth dayglow, nightglow, sunlit limb, and nighttime limb. Samples of the data are presented later in reduced form. At this point, it is important that the reader understand the geometry and the method of converting the raw data into a measure of the earth's radiance.

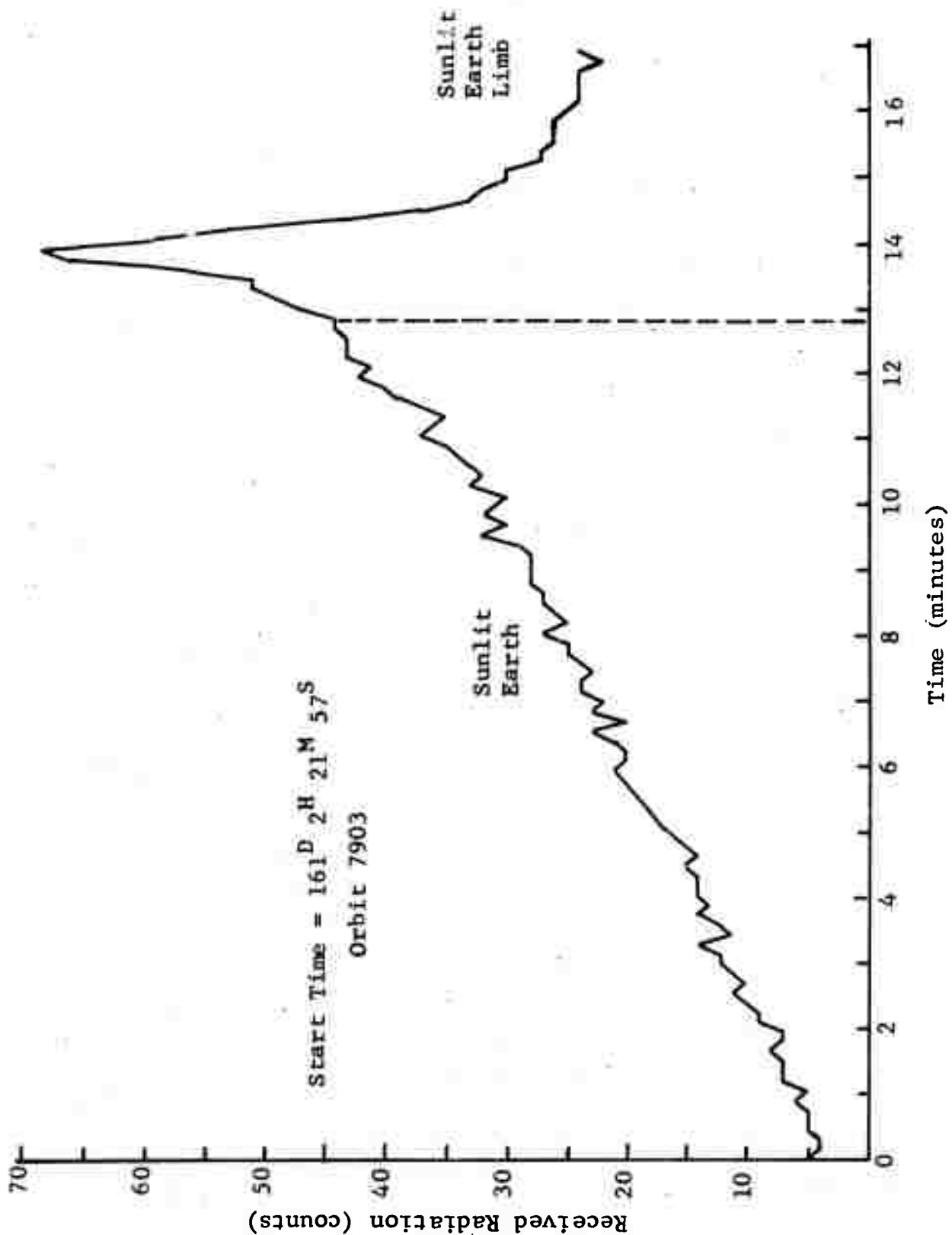


Fig. 5 Received Radiation Measured with 1250ⁱ Filter

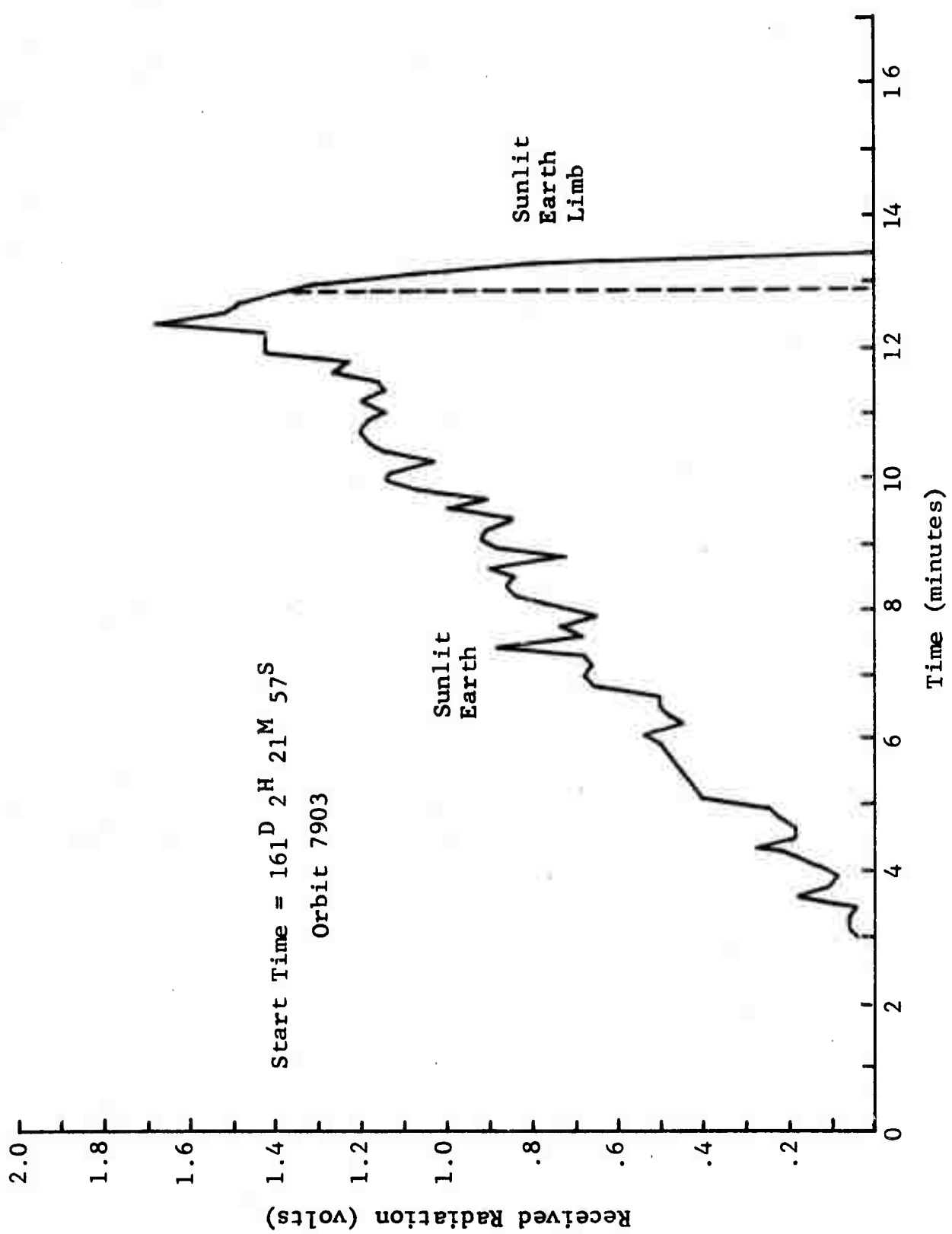


Fig. 6 Received Radiation Measured with 1920 \AA Filter

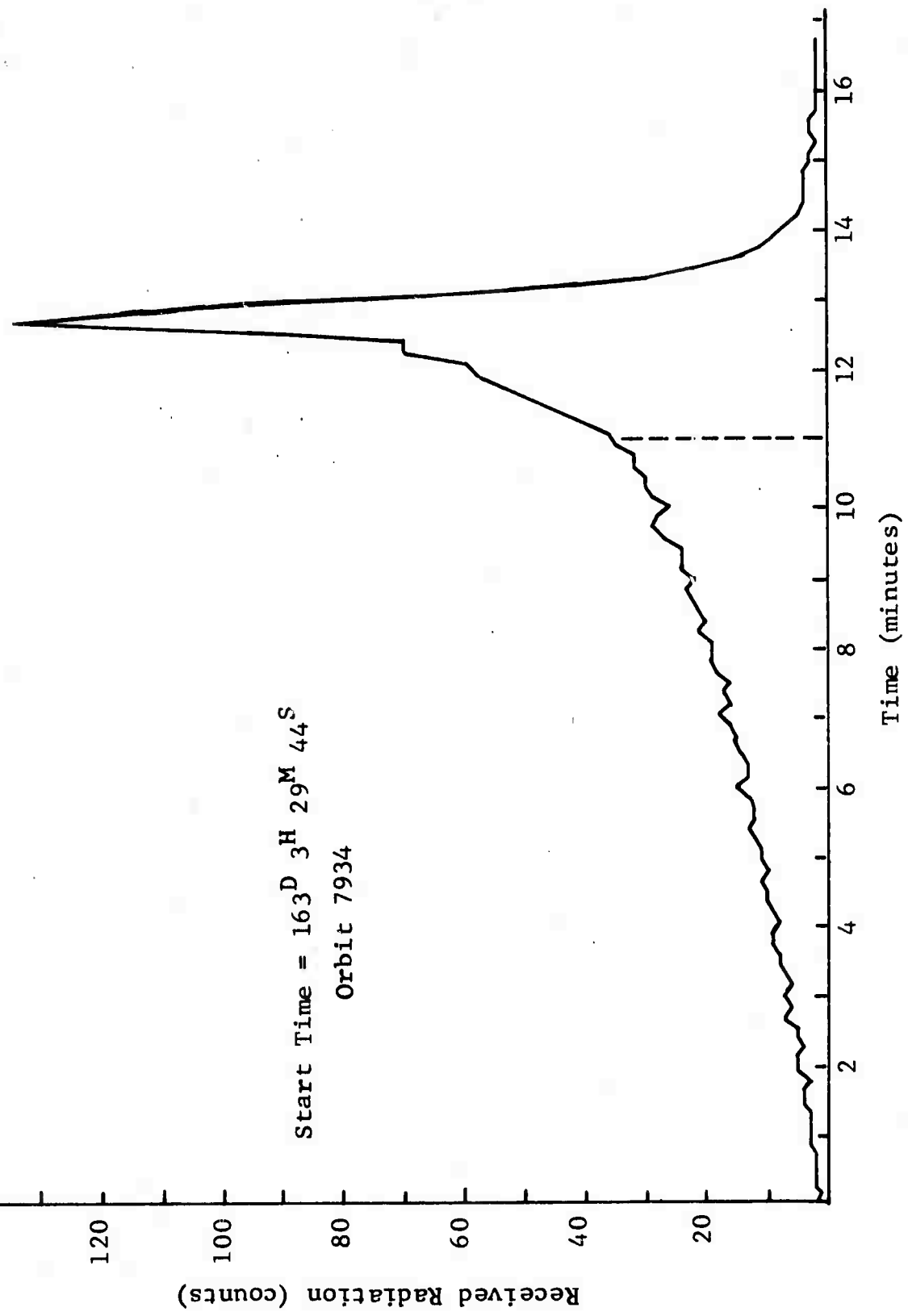


Fig. 7 Received Radiation Measured with 1500Å Filter

Consider a typical viewing situation such as shown in Fig. 8. The total received radiation is the sum of the contributions from each portion of the atmosphere along the line of sight vector, s , that is

$$I_T(s) = \int_{I_r(s=0)}^{I_r(s=\infty)} dI_r(s) \quad (1)$$

where $s = 0$ is the point of intersection with the earth's surface and the upper limit is at $s = \infty$ if the detector is outside the atmosphere. The increment $dI_r(s)$ is the radiation received from emissions originating at a distance, s , from a layer of atmosphere of thickness, ds . Assuming that the source of radiation fills the field of view, we have

$$A_o dI_r(s) = A_e(s) B(s) I(s) T(s) ds \quad (2)$$

A_o = collecting area of the optics (cm^2)

$A_e(s)$ = the area of atmosphere at a distance (s), that contributes to the received radiation (cm^2)

$B(s)$ = the solid angle subtended by the detector at a distance s (steradians)

$T(s)$ = the transmission of the atmosphere from s to the detector

$I(s)$ = atmospheric radiance at s ($\text{w}/\text{cm}^3\text{-ster}$)

Now, by definition

$$A_e(s) B(s) = A_o^\alpha \quad (3)$$

where

α = field of view of the detector (steradians)

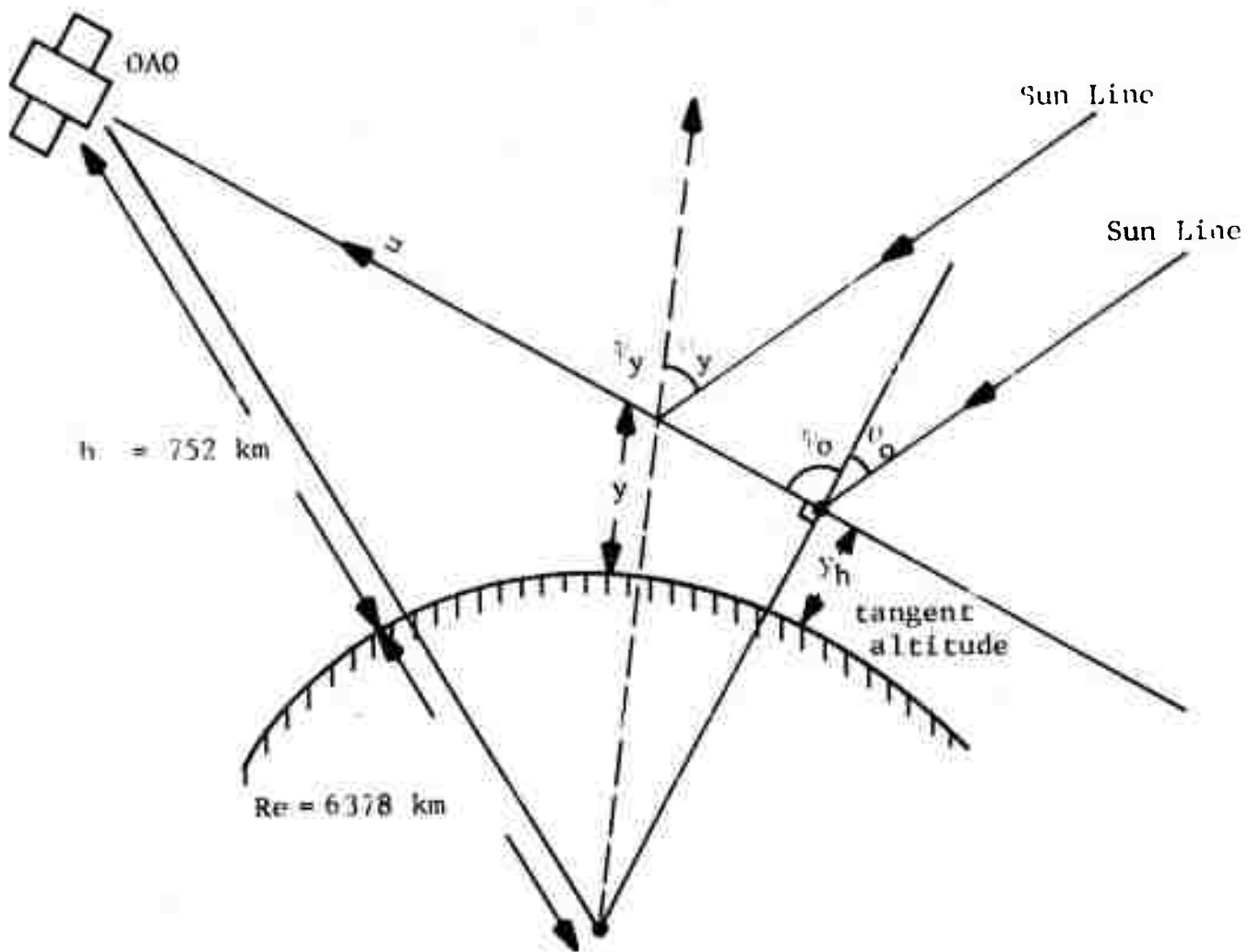


Fig. 8 Typical Viewing Geometry

Hence the radiation received by the detector from a source at a distance s , is

$$dI_r(s) = \alpha I(s)T(s)ds \quad (4)$$

Integrating along the line of sight, the total received radiation is

$$I_T = \alpha \int_{s=0}^{\infty} I(s)T(s)ds \quad (5)$$

$$= \alpha I_B \quad (6)$$

I_B is the equivalent radiance of the earth in $w/cm^2\text{-ster}$. It is dependent on the angle between the LOS and the local zenith and also the position of the sun. The earth's radiance normally is defined by the situation when both the LOS and the sun line lie along the local spacecraft zenith. A method for obtaining this particular value of the radiance from the measured intensities is discussed in the next section, together with some results of this reduction.

The equivalent radiance can be calculated from the measured irradiance values and gives a good indication of the magnitude of the true radiance. Therefore, all measurements have been reduced to their equivalent radiance. The viewing geometry and equivalent radiance for each data sample have been placed on computer cards and tape. Each line of the printout from the cards and tape contains

- 1) the run number
- 2) a day or night designation (D or N) to indicate the condition of the area on the earth viewed at the time of the sample
- 3) the GMT time of the measurement in days, hours, minutes, and seconds
- 4) the tangent altitude (TAN.ALT) given in kilometers

- 5) the solar-zenith angle (SUN.ANG), which is the angle between the sun line and the local vertical through the earth at either the intersection point of the LOS with the earth's surface or the tangent altitude point
- 6) the line-of-sight/zenith angle (OBS ANG), which is the angle between the line of sight and the local vertical at the point indicated in 5)
- 7) the Rayleigh scattering angle (SCAT ANG), which is the angle between the LOS vector and the sun line
- 8) the longitude (LON) and latitude (LAT) of either the intersection point of the LOS with the earth's surface or the tangent altitude point
- 9) the equivalent radiance values from the 1250, 1380, 1920, 2380, 2460, and 2980 \AA filter photometers of the WEP.

The data samples are given at 3-minute intervals when the dark earth is being observed, at 1-minute intervals for sunlit observations, and every 10 seconds for measurements of the earth limb when the viewing does not intersect the earth's surface. The reduced data for all meaningful observations are given in Table 5. This table represents a computer printout of the data stored on magnetic tape.

TABLE 5

PRINTOUT OF REDUCED OAO DATA

THIS TAPE CONTAINS A SUMMARY OF THE ULTRAVIOLET EARTH BACKGROUND MEASUREMENTS THAT WERE MADE BY THE GRUMMAN AEROSPACE CORPORATION USING THE WISCONSIN EXPERIMENT PACKAGE OF OAO A-2. INFORMATION ON THE VIEWING GEOMETRY AND THE MEASURED RADIANCE VALUES FOR THE PHOTOMETERS ARE GIVEN FOR EACH DATA SAMPLE. THE MEASUREMENTS WERE OBTAINED DURING THE GMT DAYS 161-164 AND 268 OF 1970 AND FOR DAYS 82-146, 215 AND 225 OF 1971.

EACH LINE OF PRINTOUT CONTAINS

- (1) THE RUN NUMBER
- (2) A DAY OR NIGHT DESIGNATION. (D CR N) TO INDICATE THE CONDITION OF THE AREA ON THE EARTH VIEWED AT THE TIME OF THE RUN.
- (3) THE GMT TIME OF THE MEASUREMENT IN DAYS, HOURS, MINUTES AND SECONDS.
- (4) THE TANGENT ALTITUDE (TAN. ALT) GIVEN IN KILOMETERS WHICH IS THE MINIMUM HEIGHT THAT THE LINE OF SIGHT MAKES WITH THE EARTH'S SURFACE.
- (5) THE SOLAR-ZENITH ANGLE (SUN ANG) WHICH IS THE ANGLE BETWEEN THE SUN LINE AND THE LOCAL VERTICAL THROUGH THE EARTH AT EITHER THE INTERSECTION POINT OF THE LOS WITH THE EARTH'S SURFACE OR THE THE TANGENT ALTITUDE POINT.
- (6) THE LINE OF SIGHT-ZENITH ANGLE (OBS ANG) WHICH IS THE ANGLE BETWEEN THE LINE OF SIGHT AND THE LOCAL VERTICAL AT THAT POINT.
- (7) THE RAYLEIGH SCATTERING ANGLE (SCAT ANG) WHICH IS THE ANGLE BETWEEN THE LINE OF SIGHT VECTOR AND THE SUN LINE.
- (8) THE LONGITUDE (LON) AND LATITUDE (LAT) OF THE OAO POSITION.
- (9) THE LONGITUDE (LON) AND LATITUDE (LAT) OF EITHER THE INTERSECTION POINT OF THE LOS WITH THE EARTH'S SURFACE OR THE TANGENT ALTITUDE POINT.
- (10) THE MEASURED RADIANCE VALUES FROM THE 1250A, 1380A, 1500A, 1920A, 2380A, 2460A AND 2980A FILTER PHOTOMETERS OF THE WISCONSIN EXPERIMENT PACKAGE. THESE VALUES WERE OBTAINED BY DIVIDING THE MEASURED IRRADIANCE BY THE FIELD OF VIEW OF THE WEP PHOTOMETERS (6.646×10^{-6} STERADIANS). THEY ARE THEREFORE EQUIVALENT RADIANCE VALUES.

SUN		TAI		SCAT		DAD		CBS		C&C		29CCA 1PE9.2	
GMT	DAY	S	ALT	ANG	ANS	LON	LAT	LBN	LAT	C&C	C&C	C&C	C&C
12 161	1 12 57	2 1 34.3	36.1	77.7	25	-1	21	1 4.99E-38	0.0	0.0	0.0	0.0	0.0
12 161	1 15 57	0 1 22.1	30.8	87.7	34	6	31	8 4.99E-28	0.0	0.0	0.0	0.0	0.0
12 161	1 18 57	0 1 10.1	29.5	55.3	42	12	43	15 4.99E-28	0.0	0.0	0.0	0.0	0.0
12 161	1 21 57	2 97.9	33.5	112.7	51	17	50	21 1.09E-07	0.0	0.0	0.0	0.0	0.0
12 161	1 22 57	0 33.9	35.6	116.3	54	19	54	23 1.55E-07	0.0	0.0	0.0	0.0	0.0
12 161	1 27 57	2 73.0	50.1	174.6	75	27	74	33 5.23E-07	0.0	0.0	0.0	0.0	0.0
12 161	1 28 57	2 58.7	52.7	136.5	73	29	78	35 5.71E-07	0.0	0.0	0.0	0.0	0.0
12 161	1 29 57	3 60.2	57.5	137.4	77	30	83	37 6.18E-07	0.0	0.0	0.0	0.0	0.0
12 161	1 30 57	2 59.5	61.7	137.3	81	31	89	39 6.89E-07	0.0	0.0	0.0	0.0	0.0
12 161	1 31 53	0 55.0	65.0	125.3	94	32	94	43 7.85E-07	0.0	0.0	0.0	0.0	0.0
12 161	1 32 53	2 49.6	71.1	132.3	93	33	101	42 8.80E-07	0.0	0.0	0.0	0.0	0.0
12 161	1 33 53	2 43.3	77.7	127.7	92	33	113	44 9.98E-07	0.0	0.0	0.0	0.0	0.0
12 161	1 34 53	3 56	33.5	92.0	96	34	127	47 1.14E-06	0.0	0.0	0.0	0.0	0.0
12 161	1 35 53	3 64	33.3	95.0	116.3	97	34	127	46 1.21E-06	0.0	0.0	0.0	0.0
12 161	1 35 13	62	33.0	90.0	115.4	97	34	127	45 1.25E-06	0.0	0.0	0.0	0.0
12 161	1 35 23	122	32.8	90.5	115.1	98	34	127	45 1.26E-06	0.0	0.0	0.0	0.0
12 161	1 35 33	146	32.5	90.5	114.3	99	34	127	45 1.64E-06	0.0	0.0	0.0	0.0
12 161	1 35 47	173	32.3	90.5	114.5	97	34	127	45 1.68E-06	0.0	0.0	0.0	0.0
12 161	1 35 52	199	32.0	90.5	114.2	100	35	127	45 1.43E-06	0.0	0.0	0.0	0.0
12 161	1 36 2	224	31.4	90.5	113.3	101	35	127	45 1.26E-06	0.0	0.0	0.0	0.0
12 161	1 36 17	249	31.5	92.0	113.7	101	35	127	44 1.07E-06	0.0	0.0	0.0	0.0
12 161	1 36 23	274	31.3	90.5	113.4	102	35	127	44 5.27E-07	0.0	0.0	0.0	0.0
12 161	1 36 31	297	31.1	93.0	113.1	103	35	127	44 8.08E-07	0.0	0.0	0.0	0.0
12 161	1 36 43	321	30.8	90.5	112.8	104	35	126	43 7.85E-07	0.0	0.0	0.0	0.0
12 161	1 36 53	343	32.6	90.5	112.5	104	35	128	43 7.61E-07	0.0	0.0	0.0	0.0
12 161	1 37 53	369	26.5	91.5	112.9	103	35	128	41 6.18E-07	0.0	0.0	0.0	0.0
20 161	1 37 53	469	30.1	140.0	39.7	74.3	356	-3 4.59E-08	0.0	0.0	0.0	0.0	0.0
20 161	2 51 46	0 95.6	34.9	115.4	27	19	27	23 1.24E-07	0.0	0.0	0.0	0.0	0.0
20 161	2 54 45	0 127.9	33.0	52.9	5	3	1	5 4.99E-08	0.0	0.0	0.0	0.0	0.0
20 161	2 57 46	0 115.8	33.0	94.1	13	9	11	12 6.89E-08	0.0	0.0	0.0	0.0	0.0
20 161	3 4 46	0 123.7	31.5	106.3	21	15	20	18 9.27E-08	0.0	0.0	0.0	0.0	0.0
20 161	3 5 46	0 123.7	32.3	42.5	127.3	37	24	29 3.33E-07	0.0	0.0	0.0	0.0	0.0
20 161	3 6 59	0 145	39.6	111.1	41	26	43	31 4.40E-07	0.0	0.0	0.0	0.0	0.0
20 161	3 7 59	0 146	34.9	115.4	27	19	27	33 4.99E-07	0.0	0.0	0.0	0.0	0.0
20 161	3 8 59	0 146	39.5	134.2	44	27	48	35 5.47E-07	0.0	0.0	0.0	0.0	0.0
20 161	3 9 59	0 146	37.1	91.5	119.5	30	21	25 1.9CE-07	0.0	0.0	0.0	0.0	0.0
20 161	3 10 59	0 146	37.4	39.7	123.6	33	22	34 2.62E-07	0.0	0.0	0.0	0.0	0.0
20 161	3 11 59	0 146	32.3	42.5	127.3	37	24	38 3.33E-07	0.0	0.0	0.0	0.0	0.0
20 161	3 12 59	0 146	37.4	46.2	76.9	128.5	66	33 83	43 9.98E-07	0.0	0.0	0.0	0.0
20 161	3 13 59	0 146	33.8	90.5	116.0	70	34	101 47 1.12E-06	0.0	0.0	0.0	0.0	0.0
20 161	3 14 59	16	33.8	90.5	116.0	71	34	101 47 1.18E-06	0.0	0.0	0.0	0.0	0.0
20 161	3 15 59	45	33.5	90.5	116.0	72	34	102 46 1.26E-06	0.0	0.0	0.0	0.0	0.0

RUN	D	GMT	TAN	SUR	DBS	SCAT	DAU	CBS	ANG	LON	LAT	1250A	1300A	1500A	1700A	2333A	2460A	1DE9.2	1DE9.2	2900A	1PE9.2	1PE9.2
ND.	N	DAY	H	4	5	ALT																
14	A2	14	13	13	13	13	14	14	F6.1	F6.1	F6.1	9	9	9	9	9	9	9	9	9	9	9
6D	161	18	4	55	5	56	2	31.3	39.0	117.2	161	22	161	25	0.0	2.94E-CB	C.C	0.0	0.0	0.0	0.0	0.0
6D	161	18	5	56	5	56	2	31.3	39.0	121.3	164	22	154	27	0.0	6.5AE-CB	C.C	0.0	0.0	0.0	0.0	0.0
6D	161	18	6	55	6	55	2	37.2	41.5	125.2	167	24	168	23	0.0	1.12E-C7	C.C	0.0	0.0	0.0	0.0	0.0
6D	161	19	7	56	7	56	2	42.0	44.2	129.3	170	25	172	31	0.0	1.49E-C7	0.0	0.0	0.0	0.0	0.0	0.0
6D	161	18	8	56	8	56	2	78.8	87.2	132.0	174	27	175	33	0.0	1.9CE-C7	0.0	0.0	0.0	0.0	0.0	0.0
6D	161	18	9	56	9	56	2	74.6	80.4	134.7	177	28	161	34	0.0	2.25E-C7	0.0	0.0	0.0	0.0	0.0	0.0
6D	161	18	10	56	10	56	2	72.2	53.8	136.7	131	29	195	25	0.0	2.6CE-C7	0.0	0.0	0.0	0.0	0.0	0.0
6D	161	18	11	56	11	56	2	65.7	57.5	137.7	135	31	193	33	0.0	3.11E-C7	0.0	0.0	0.0	0.0	0.0	0.0
6D	161	18	12	56	12	56	2	51.1	61.5	137.7	138	32	196	33	0.0	3.81E-C7	0.0	0.0	0.0	0.0	0.0	0.0
6D	161	18	13	56	13	56	2	56.2	55.5	136.4	192	33	202	41	0.0	4.15E-C7	0.0	0.0	0.0	0.0	0.0	0.0
6D	161	19	14	56	14	56	2	53.9	72.9	133.5	196	33	205	42	0.0	4.85E-C7	0.0	0.0	0.0	0.0	0.0	0.0
6D	161	18	15	56	15	56	2	44.8	77.2	128.6	202	34	217	44	0.0	5.71E-C7	0.0	0.0	0.0	0.0	0.0	0.0
6D	161	18	16	56	16	56	2	34.5	90.0	116.6	204	34	235	47	0.0	6.75E-C7	2.0	0.0	0.0	0.0	0.0	0.0
7D	161	19	42	1	42	1	2	124.1	33.7	128.4	129	17	128	25	0.0	1.21E-C8	0.0	0.0	0.0	0.0	0.0	0.0
7D	161	19	44	1	44	1	2	132.1	35.1	112.6	132	18	131	23	0.0	1.73E-C8	0.0	0.0	0.0	0.0	0.0	0.0
7D	161	19	45	1	45	1	2	96.0	36.6	116.3	205	20	139	25	0.0	1.73E-C8	C.C	0.0	0.0	0.0	0.0	0.0
7D	161	19	46	1	46	1	2	91.9	38.6	120.3	138	22	139	27	0.0	5.36E-C8	C.C	0.0	0.0	0.0	0.0	0.0
7D	161	19	47	1	47	1	2	87.8	41.3	124.3	141	24	142	29	0.0	9.69E-C8	0.0	0.0	0.0	0.0	0.0	0.0
7D	161	19	48	1	48	1	2	93.7	44.0	128.4	145	25	146	31	0.0	1.42E-07	2.0	0.0	0.0	0.0	0.0	0.0
7D	161	19	49	1	49	1	2	79.5	46.9	131.7	148	27	151	33	0.0	1.73E-C7	0.0	0.0	0.0	0.0	0.0	0.0
7D	161	19	50	1	50	1	2	75.2	50.0	134.4	152	28	155	34	0.0	2.08E-C7	0.0	0.0	0.0	0.0	0.0	0.0
7D	161	19	51	1	51	1	2	75.9	53.4	136.5	155	29	160	35	0.0	2.60E-C7	0.0	0.0	0.0	0.0	0.0	0.0
7D	161	19	52	1	52	1	2	56.4	57.1	137.7	159	30	165	38	0.0	3.11E-C7	0.0	0.0	0.0	0.0	0.0	0.0
7D	161	19	53	1	53	1	2	51.8	61.0	137.8	163	32	170	39	0.0	3.46E-C7	0.0	0.0	0.0	0.0	0.0	0.0
7D	161	19	54	1	54	1	2	57.0	65.2	136.7	156	32	176	41	0.0	4.15E-C7	0.0	0.0	0.0	0.0	0.0	0.0
7D	161	19	55	1	55	1	2	51.7	51.7	134.2	170	33	183	42	0.0	4.67E-C7	C.C	0.0	0.0	0.0	0.0	0.0
7D	161	19	56	1	56	1	2	45.0	76.3	129.4	174	34	191	44	0.0	5.19E-C7	0.0	0.0	0.0	0.0	0.0	0.0
7D	161	19	57	1	57	1	2	35.8	88.3	116.4	178	34	207	47	0.0	6.23E-C7	0.0	0.0	0.0	0.0	0.0	0.0
8D	161	21	23	9	9	9	2	124.5	33.9	1C8.2	104	17	102	22	0.0	1.21E-C8	0.0	0.0	0.0	0.0	0.0	0.0
8D	161	21	24	9	9	9	2	103.5	35.1	112.4	107	18	106	23	0.0	1.21E-C8	0.0	0.0	0.0	0.0	0.0	0.0
8D	161	21	25	9	9	9	2	96.4	36.8	116.6	110	2C	105	25	0.0	1.73E-C8	C.C	0.0	0.0	0.0	0.0	0.0
8D	161	21	26	9	9	9	2	92.3	38.9	120.6	113	22	113	27	0.0	4.33E-C8	0.0	0.0	0.0	0.0	0.0	0.0
8D	161	21	27	9	9	9	2	98.2	41.0	124.5	116	24	116	36	C.C	2.60E-C7	0.0	0.0	0.0	0.0	0.0	0.0
8D	161	21	28	9	9	9	2	84.1	43.9	128.2	119	25	121	31	0.0	9.17E-C8	0.0	0.0	0.0	0.0	0.0	0.0
8D	161	21	29	9	9	9	2	79.9	46.7	131.5	123	27	125	33	0.0	1.32E-C7	0.0	0.0	0.0	0.0	0.0	0.0
8D	161	21	30	9	9	9	2	75.6	57.5	136.8	141	32	154	41	0.0	1.68E-C7	0.0	0.0	0.0	0.0	0.0	0.0
8D	161	21	31	9	9	9	2	52.3	69.8	134.3	145	33	157	42	0.0	2.25E-C7	0.0	0.0	0.0	0.0	0.0	0.0
8D	161	21	32	9	9	9	2	46.3	75.7	129.9	149	34	165	44	0.0	4.33E-C7	0.0	0.0	0.0	0.0	0.0	0.0
8D	161	21	33	9	9	9	2	37.6	85.8	120.8	153	34	175	46	C.C	5.02E-C7	0.0	0.0	0.0	0.0	0.0	0.0
8D	161	21	34	9	9	9	2	102.5	34.5	110.3	80	18	79	22	0.0	6.23E-C7	0.0	0.0	0.0	0.0	0.0	0.0
9D	161	21	35	9	9	9	2	98.4	314.5	114.5	83	19	82	24	0.0	1.21E-C8	0.0	0.0	0.0	0.0	0.0	0.0
9D	161	21	36	9	9	9	2	94.4	37.8	118.6	86	21	85	26	0.0	1.73E-08	0.0	0.0	0.0	0.0	0.0	0.0
9D	161	21	37	9	9	9	2	90.3	40.0	122.6	89	23	90	28	0.0	3.44E-C8	0.0	0.0	0.0	0.0	0.0	0.0
9D	161	21	38	9	9	9	2	86.2	42.5	126.4	92	24	94	30	0.0	7.44E-C8	0.0	0.0	0.0	0.0	0.0	0.0
9D	161	21	39	9	9	9	2	82.0	45.3	129.9	96	26	98	32	0.0	1.21E-C7	0.0	0.0	0.0	0.0	0.0	0.0
9D	161	21	40	9	9	9	2	77.8	48.3	132.9	99	27	102	33	0.0	1.56E-C7	0.0	0.0	0.0	0.0	0.0	0.0

DUN	D	GMT	TAN	SUN	OBS	SCAT	340	385	ANG	LAT	LON	LAT	1250A	1380A	1500A	1620A	1PE9.2	1PE9.2	2380A	2460A	2900A	1PE9.2	1PE9.2				
160	162	19	11	8	95.9	49.0	132.1	155	28	157	34	0.0	32	0.0	2.15E-08	C-C	C-0	0.0	0.0	0.0	0.0	0.0	0.0	0.0			
160	162	19	12	9	96.6	50.3	134.7	159	29	162	36	0.0	27	153	32	C-C	2.14E-08	5.82E-07	0.0	0.0	0.0	0.0	0.0	0.0	0.0		
160	162	19	13	5	147.0	48.6	78.3	82	-2	75	0.0	0.0	0.0	0.0	0.0	0.0	3.64E-C8	1.C5E-C6	0.0	0.0	0.0	0.0	0.0	0.0	0.0		
170	162	20	35	37	91.3	134.8	41.2	84.7	90	4	85	7	0.0	0.0	0.0	0.0	3.67E-C5	0.0	0.0	0.0	0.0	0.0	0.0	0.0	0.0		
170	162	20	41	57	112.7	122.7	36.7	93.7	98	10	95	13	0.0	0.0	0.0	0.0	3.67E-C5	0.0	0.0	0.0	0.0	0.0	0.0	0.0	0.0		
170	162	20	44	57	112.6	124.6	34.6	124.3	125	16	104	20	0.0	0.0	0.0	0.0	3.67E-C5	0.0	0.0	0.0	0.0	0.0	0.0	0.0	0.0		
170	162	20	47	57	92.5	38.6	116.7	116	22	115	26	0.0	0.0	0.0	0.0	0.0	0.0	0.0	0.0	0.0	0.0	0.0	0.0	0.0	0.0		
170	162	20	48	57	94.5	40.3	126.7	119	23	115	29	0.0	0.0	0.0	0.0	0.0	0.0	0.0	0.0	0.0	0.0	0.0	0.0	0.0	0.0		
170	162	20	49	57	95.4	42.4	124.5	122	25	123	30	0.0	0.0	0.0	0.0	0.0	0.0	0.0	0.0	0.0	0.0	0.0	0.0	0.0	0.0		
170	162	20	50	57	86.2	44.7	128.1	125	26	127	32	0.0	0.0	0.0	0.0	0.0	0.0	0.0	1.82E-C6	5.82E-08	0.0	0.0	0.0	0.0	0.0	0.0	
170	162	20	51	57	92.1	47.3	131.3	129	28	131	34	0.0	0.0	0.0	0.0	0.0	0.0	0.0	2.48E-C2	5.82E-C7	0.0	0.0	0.0	0.0	0.0	0.0	
170	162	20	52	57	77.8	50.2	134.1	132	29	135	35	0.0	0.0	0.0	0.0	0.0	0.0	0.0	3.64E-08	1.19E-06	0.0	0.0	0.0	0.0	0.0	0.0	
180	162	22	17	42	142.7	44.7	81.6	65	1	55	0.0	0.0	0.0	0.0	0.0	0.0	0.0	3.97E-09	C-C	C-0	0.0	0.0	0.0	0.0	0.0	0.0	
180	162	22	23	42	128.6	38.7	85.2	69	8	65	12	0.0	0.0	0.0	0.0	0.0	0.0	0.0	3.97E-09	0.0	0.0	0.0	0.0	0.0	0.0	0.0	
180	162	22	23	42	115.6	36.5	99.4	77	14	74	17	0.0	0.0	0.0	0.0	0.0	0.0	0.0	3.97E-09	C-C	0.0	0.0	0.0	0.0	0.0	0.0	
180	162	22	26	42	104.5	37.0	111.5	86	19	84	23	0.0	0.0	0.0	0.0	0.0	0.0	0.0	3.97E-09	0.0	0.0	0.0	0.0	0.0	0.0	0.0	
180	162	22	27	42	125.5	38.1	115.5	39	21	68	26	0.0	0.0	0.0	0.0	0.0	0.0	0.0	3.97E-09	C-C	0.0	0.0	0.0	0.0	0.0	0.0	
180	162	22	28	42	96.4	39.7	118.9	92	23	92	28	0.0	0.0	0.0	0.0	0.0	0.0	0.0	3.97E-09	0.0	0.0	0.0	0.0	0.0	0.0	0.0	
190	162	22	29	42	92.3	41.6	122.5	95	24	95	29	0.0	0.0	0.0	0.0	0.0	0.0	0.0	7.94E-09	C-C	0.0	0.0	0.0	0.0	0.0	0.0	
180	162	22	30	42	88.2	43.7	126.5	99	26	99	31	0.0	0.0	0.0	0.0	0.0	0.0	0.0	7.78E-09	C-C	0.0	0.0	0.0	0.0	0.0	0.0	
180	162	22	31	42	94.1	46.2	129.9	102	27	104	33	0.0	0.0	0.0	0.0	0.0	0.0	0.0	2.65E-08	2.62E-07	0.0	0.0	0.0	0.0	0.0	0.0	
190	163	0	4	54	112.7	36.1	103.2	55	16	52	19	0.0	0.0	0.0	0.0	0.0	0.0	0.0	3.97E-09	0.0	0.0	0.0	0.0	0.0	0.0	0.0	
190	163	0	7	54	175.6	35.3	115.5	64	21	63	26	0.0	0.0	0.0	0.0	0.0	0.0	0.0	3.97E-09	C-C	0.0	0.0	0.0	0.0	0.0	0.0	
190	163	0	8	54	96.5	39.6	119.3	67	23	66	28	0.0	0.0	0.0	0.0	0.0	0.0	0.0	6.62E-09	C-C	0.0	0.0	0.0	0.0	0.0	0.0	
190	163	0	9	54	92.5	41.7	122.3	70	24	76	30	0.0	0.0	0.0	0.0	0.0	0.0	0.0	7.78E-09	C-C	0.0	0.0	0.0	0.0	0.0	0.0	
190	163	0	10	54	88.3	43.8	126.5	73	26	74	31	0.0	0.0	0.0	0.0	0.0	0.0	0.0	1.21E-08	C-C	0.0	0.0	0.0	0.0	0.0	0.0	
190	163	0	11	54	84.2	46.3	125.5	77	27	78	33	0.0	0.0	0.0	0.0	0.0	0.0	0.0	2.65E-08	1.75E-07	0.0	0.0	0.0	0.0	0.0	0.0	
190	163	0	12	54	80.2	49.2	133.2	80	29	83	35	0.0	0.0	0.0	0.0	0.0	0.0	0.0	3.14E-C8	5.82E-07	0.0	0.0	0.0	0.0	0.0	0.0	
200	163	1	48	45	97.9	39.5	117.9	41	22	40	27	0.0	0.0	0.0	0.0	0.0	0.0	0.0	3.97E-09	C-C	0.0	0.0	0.0	0.0	0.0	0.0	
200	163	1	49	45	93.7	41.2	121.3	44	24	44	29	0.0	0.0	0.0	0.0	0.0	0.0	0.0	8.28E-C9	C-C	0.0	0.0	0.0	0.0	0.0	0.0	
200	163	1	50	45	99.6	43.3	125.5	47	26	44	31	0.0	0.0	0.0	0.0	0.0	0.0	0.0	1.21E-08	C-C	0.0	0.0	0.0	0.0	0.0	0.0	
200	163	1	51	49	85.5	45.6	129.5	51	27	52	33	0.0	0.0	0.0	0.0	0.0	0.0	0.0	2.48E-08	2.91E-07	0.0	0.0	0.0	0.0	0.0	0.0	
200	163	1	52	49	91.3	48.3	132.2	54	28	56	35	0.0	0.0	0.0	0.0	0.0	0.0	0.0	3.31E-08	6.40E-07	0.0	0.0	0.0	0.0	0.0	0.0	
200	163	1	53	49	77.1	51.1	134.8	58	30	61	36	0.0	0.0	0.0	0.0	0.0	0.0	0.0	3.97E-08	9.89E-07	0.0	0.0	0.0	0.0	0.0	0.0	
200	163	1	54	49	72.8	54.3	136.3	61	31	66	38	0.0	0.0	0.0	0.0	0.0	0.0	0.0	4.80E-08	1.34E-06	0.0	0.0	0.0	0.0	0.0	0.0	
200	163	1	55	49	68.3	57.6	138.0	65	32	71	39	0.0	0.0	0.0	0.0	0.0	0.0	0.0	5.56E-08	2.04E-06	0.0	0.0	0.0	0.0	0.0	0.0	
200	163	1	56	49	63.7	61.3	138.1	69	33	76	41	0.0	0.0	0.0	0.0	0.0	0.0	0.0	7.28E-08	2.76E-06	0.0	0.0	0.0	0.0	0.0	0.0	
200	163	1	57	49	58.9	65.4	137.1	73	33	82	42	0.0	0.0	0.0	0.0	0.0	0.0	0.0	7.94E-08	3.17E-06	0.0	0.0	0.0	0.0	0.0	0.0	
200	163	1	58	49	53.9	70.0	134.6	77	34	89	43	0.0	0.0	0.0	0.0	0.0	0.0	0.0	9.93E-08	3.78E-06	0.0	0.0	0.0	0.0	0.0	0.0	
200	163	1	59	49	47.9	54.6	130.4	81	34	97	44	0.0	0.0	0.0	0.0	0.0	0.0	0.0	1.16E-07	3.78E-06	0.0	0.0	0.0	0.0	0.0	0.0	
210	163	3	26	44	9.0	107.2	37.1	105.0	8	18	6	23	0.0	0.0	0.0	0.0	0.0	0.0	0.0	3.97E-09	0.0	0.0	0.0	0.0	0.0	0.0	0.0
210	163	3	27	44	1.3	1.3	38.2	112.9	11	20	10	25	0.0	0.0	0.0	0.0	0.0	0.0	0.0	3.97E-09	0.0	0.0	0.0	0.0	0.0	0.0	0.0
210	163	3	28	44	9.0	99.1	39.0	116.9	14	22	14	27	0.0	0.0	0.0	0.0	0.0	0.0	0.0	3.97E-09	C-C	0.0	0.0	0.0	0.0	0.0	0.0
210	163	3	29	44	95.0	40.8	120.7	18	24	17	29	0.0	0.0	0.0	0.0	0.0	0.0	0.0	5.79E-09	C-C	0.0	0.0	0.0	0.0	0.0	0.0	
210	163	3	30	44	90.9	42.8	124.5	21	25	21	31	0.0	0.0	0.0	0.0	0.0	0.0	0.0	1.18E-08	0.0	0.0	0.0	0.0	0.0	0.0	0.0	
210	163	3	31	44	86.8	45.0	128.1	24	27	25	32	0.0	0.0	0.0	0.0	0.0	0.0	0.0	1.82E-08	2.91E-07	0.0	0.0	0.0	0.0	0.0	0.0	
210	163	3	32	44	82.6	47.6	131.3	23	28	30	34	0.0	0.0	0.0	0.0	0.0	0.0	0.0	2.48E-08	5.24E-07	0.0	0.0	0.0	0.0	0.0	0.0	
210	163	3	33	44	78.4	50.3	134.3	31	29	34	36	0.0	0.0	0.0	0.0	0.0	0.0	0.0	3.31E-08	1.02E-06	0.0	0.0	0.0	0.0	0.0	0.0	

QUN	D	SMT	TAN	SUN	39S	SCAT	JAD	OBS	4NG	4NG	LCN	LAT	LEN	LAT	1250A	1380A	150CA	192CA	238JA	2460A	1PE9.2	1PE9.2	1PE9.2	1PE9.2	2900A	1PE9.2		
ND.	N	DAY	H	4	5																							
14	42	16	13	12	13	13	13	13	13	13	13	13	13	13	13	13	13	13	13	13	13	13	13	13	13	13	13	
21D	162	7	25	44	0	69.7	56.7	137.7	39	32	44	39	0.0															
21D	163	8	36	44	0	65.2	65.2	138.2	43	32	43	42	0.0															
21D	163	8	37	44	0	50.5	64.2	137.5	47	33	55	42	2.0															
21D	163	8	38	44	0	55.4	68.6	135.5	51	34	62	63	0.0															
21D	163	8	39	44	0	49.9	73.8	131.3	55	34	65	44	0.0															
21D	163	8	40	44	0	42.9	81.0	125.6	59	35	79	45	0.0															
21D	163	8	41	41	0	75	35.1	90.5	116.2	63	35	93	47	0.0														
21D	163	8	41	51	0	131	34.8	95.5	115.3	63	35	93	47	0.0														
21D	163	8	42	1	0	127	34.5	90.6	115.5	64	35	93	46	0.0														
21D	163	8	42	11	0	152	34.2	90.0	114.1	65	35	93	46	0.0														
21D	163	8	43	1	0	279	33.2	90.3	113.7	67	35	93	45	0.0														
21D	163	8	43	11	0	292	32.5	90.6	114.3	65	35	93	46	0.0														
21D	163	8	43	21	0	314	32.3	90.0	112.7	69	35	93	46	0.0														
21D	163	8	43	21	0	336	32.0	90.3	112.4	70	35	94	43	0.0														
21D	163	8	43	41	0	247	33.1	90.3	113.7	71	35	94	43	0.0														
21D	163	8	43	51	0	279	32.8	90.6	113.4	63	35	94	44	0.0														
21D	163	8	43	51	0	292	32.5	90.6	113.1	69	35	94	44	0.0														
21D	163	8	43	52	0	314	32.3	90.0	112.7	69	35	94	44	0.0														
21D	163	8	43	52	0	336	32.0	90.3	112.4	70	35	94	43	0.0														
21D	163	8	43	52	0	357	31.7	90.2	112.1	71	35	94	43	0.0														
22D	163	5	6	50	0	157	37.2	128.7	343	18	34	23	0.0															
22D	163	5	7	50	0	157	32.5	90.6	113.7	38	2	34.6	20	34.4	25	0.0												
22D	163	5	8	50	0	159	39.2	115.5	34.9	22	34.8	27	0.0															
22D	163	5	9	50	0	159	39.6	40.3	120.4	352	24	352	29	0.0														
22D	163	5	10	50	0	159	31.7	42.7	124.2	355	25	356	31	0.0														
22D	163	5	11	50	0	173	37.3	44.3	127.7	359	27	360	32	0.0														
22D	163	5	12	50	0	159	32.2	47.4	131.0	2	28	4	34	0.0														
22D	163	5	13	50	0	159	39.0	50.1	132.9	6	29	8	36	0.0														
22D	163	5	14	50	0	159	74.7	53.1	136.1	9	30	13	37	0.0														
22D	163	5	15	50	0	159	70.3	56.3	137.7	13	32	18	39	0.0														
22D	163	5	16	50	0	159	65.8	59.9	139.2	17	32	24	40	0.0														
22D	163	5	17	50	0	161	63.7	137.7	21	33	29	41	0.0															
22D	163	5	18	50	0	161	56.1	68.1	135.9	25	34	36	43	0.0														
22D	163	5	19	50	0	161	50.6	73.1	132.4	29	34	43	44	0.0														
22D	163	5	20	50	0	161	43.9	79.9	126.6	33	35	53	45	0.0														
23D	163	6	48	54	0	100.3	39.2	116.2	323	22	322	27	0.0															
23D	163	6	49	54	0	96.2	40.7	119.9	326	23	326	29	0.0															
23D	163	6	50	54	0	92.1	42.5	123.7	330	25	330	35	0.0															
23D	163	6	51	54	0	98.0	44.7	127.3	333	27	334	32	0.0															
23D	163	6	52	54	0	83.9	47.1	130.6	336	28	338	34	0.0															
23D	163	6	53	54	0	79.7	49.8	132.5	343	29	343	36	0.0															
24D	163	8	29	6	0	100.4	39.4	116.1	298	22	297	27	0.0															
24D	163	8	30	5	0	96.3	40.9	120.3	301	24	301	29	0.0															
24D	163	8	31	6	0	92.3	42.7	123.7	304	25	305	31	0.0															
24D	163	8	32	6	0	98.2	44.8	127.3	328	27	309	32	0.0															
24D	163	8	33	6	0	94.6	47.2	130.5	311	28	313	34	0.0															
24D	163	8	34	6	0	79.8	49.3	132.5	315	29	317	36	0.0															
25D	163	10	5	59	0	101.8	39.2	114.3	372	21	270	26	0.0															
25D	163	10	59	59	0	97.7	40.5	118.8	375	23	274	28	0.0															
25D	163	10	59	59	0	93.7	42.2	122.6	278	25	278	30	0.0															
25D	163	10	59	59	0	89.5	44.2	126.2	281	26	282	32	0.0															

Run	C	Day	Sec	Sun	Tue	Wed	Thu	Fri	Sat	Obs	Scat	Dag	Lcn	Ldt	Ldn	Lst	1252A	1290A	190CA	192CA	238JA	2460A	290CA	1PE9.2	1PE9.2	1PE9.2					
47	N	28N	215	8	30	37	134	127.4	90.0	0.0	142.0	231	32	230	35	0.0	0.0	1.9AE-10	1.0C2E-10	3.0	3.37E-10	3.0	3.37E-10	3.0	3.37E-10	3.0					
47	A2	14	215	8	30	38	137	127.4	90.0	0.0	142.0	201	32	230	35	0.0	0.0	0.0	0.0	1.0C2E-10	0.0	0.0	1.0C2E-10	0.0	0.0	1.0C2E-10	0.0	0.0			
47	29D	258	17	13	31	339	127.4	90.0	0.0	142.0	201	32	230	35	0.0	0.0	1.51E-08	0.0	0.0	0.0	0.0	0.0	0.0	0.0	0.0	0.0	0.0	0.0	0.0	0.0	
47	29D	268	17	11	41	375	127.4	90.0	0.0	122.0	293	31	271	32	0.0	0.0	6.69E-09	0.0	0.0	0.0	1.74E-08	0.0	0.0	0.0	0.0	0.0	0.0	0.0	0.0	0.0	
47	29D	268	17	11	51	355	127.4	90.0	0.0	122.0	294	30	271	32	0.0	0.0	1.74E-08	0.0	0.0	0.0	2.61E-08	0.0	0.0	0.0	0.0	0.0	0.0	0.0	0.0	0.0	
47	29D	268	17	12	51	325	127.4	90.0	0.0	122.0	294	30	271	32	0.0	0.0	2.61E-08	0.0	0.0	0.0	4.34E-08	0.0	0.0	0.0	0.0	0.0	0.0	0.0	0.0	0.0	
47	29D	268	17	12	51	299	127.4	90.0	0.0	122.0	296	30	271	32	0.0	0.0	6.95E-08	0.0	0.0	0.0	0.0	0.0	0.0	0.0	0.0	0.0	0.0	0.0	0.0	0.0	0.0
47	29D	268	17	12	51	272	127.4	90.0	0.0	122.0	296	30	271	32	0.0	0.0	1.02E-07	0.0	0.0	0.0	2.52E-07	0.0	0.0	0.0	0.0	0.0	0.0	0.0	0.0	0.0	
47	29D	268	17	12	51	244	127.4	90.0	0.0	122.0	297	29	271	32	0.0	0.0	2.52E-07	0.0	0.0	0.0	4.95E-07	0.0	0.0	0.0	0.0	0.0	0.0	0.0	0.0	0.0	
47	29D	268	17	12	51	215	127.4	90.0	0.0	122.0	298	29	271	32	0.0	0.0	3.95E-07	0.0	0.0	0.0	4.95E-07	0.0	0.0	0.0	0.0	0.0	0.0	0.0	0.0	0.0	
47	29D	268	17	12	51	187	127.4	90.0	0.0	122.0	298	29	271	32	0.0	0.0	5.82E-07	0.0	0.0	0.0	4.52E-07	0.0	0.0	0.0	0.0	0.0	0.0	0.0	0.0	0.0	
47	29D	268	17	12	51	157	127.4	90.0	0.0	122.0	299	29	271	32	0.0	0.0	4.52E-07	0.0	0.0	0.0	4.08E-07	0.0	0.0	0.0	0.0	0.0	0.0	0.0	0.0	0.0	
47	29D	268	17	12	51	127	127.4	90.0	0.0	122.0	299	29	271	32	0.0	0.0	4.08E-07	0.0	0.0	0.0	4.08E-07	0.0	0.0	0.0	0.0	0.0	0.0	0.0	0.0	0.0	
47	29D	268	17	13	21	95	127.4	90.0	0.0	122.0	300	28	271	31	0.0	0.0	4.08E-07	0.0	0.0	0.0	4.08E-07	0.0	0.0	0.0	0.0	0.0	0.0	0.0	0.0	0.0	
47	29D	268	17	13	21	64	127.4	90.0	0.0	122.0	301	28	271	31	0.0	0.0	4.08E-07	0.0	0.0	0.0	4.08E-07	0.0	0.0	0.0	0.0	0.0	0.0	0.0	0.0	0.0	
47	29D	268	17	13	21	31	127.4	90.0	0.0	121.0	301	28	271	31	0.0	0.0	4.08E-07	0.0	0.0	0.0	5.21E-08	0.0	0.0	0.0	0.0	0.0	0.0	0.0	0.0	0.0	
47	30D	268	18	51	41	427	127.4	90.0	0.0	122.0	301	28	246	32	0.0	0.0	8.69E-09	0.0	0.0	0.0	6.95E-08	0.0	0.0	0.0	0.0	0.0	0.0	0.0	0.0	0.0	
47	30D	268	18	51	51	383	127.4	90.0	0.0	122.0	302	29	271	32	0.0	0.0	6.95E-08	0.0	0.0	0.0	6.95E-08	0.0	0.0	0.0	0.0	0.0	0.0	0.0	0.0	0.0	
47	30D	268	18	52	1	359	127.4	90.0	0.0	122.0	303	28	271	31	0.0	0.0	4.08E-07	0.0	0.0	0.0	4.08E-07	0.0	0.0	0.0	0.0	0.0	0.0	0.0	0.0	0.0	
47	30D	268	18	52	11	333	127.4	90.0	0.0	122.0	304	28	271	31	0.0	0.0	1.74E-08	0.0	0.0	0.0	1.74E-08	0.0	0.0	0.0	0.0	0.0	0.0	0.0	0.0	0.0	
47	30D	268	18	52	21	308	127.4	90.0	0.0	122.0	305	28	271	31	0.0	0.0	5.21E-08	0.0	0.0	0.0	5.21E-08	0.0	0.0	0.0	0.0	0.0	0.0	0.0	0.0	0.0	
47	30D	268	18	52	31	281	127.4	90.0	0.0	122.0	306	29	246	32	0.0	0.0	6.95E-08	0.0	0.0	0.0	6.95E-08	0.0	0.0	0.0	0.0	0.0	0.0	0.0	0.0	0.0	
47	30D	268	18	52	41	263	127.4	90.0	0.0	122.0	307	29	246	32	0.0	0.0	1.65E-07	0.0	0.0	0.0	2.55E-07	0.0	0.0	0.0	0.0	0.0	0.0	0.0	0.0	0.0	
47	30D	268	18	52	51	225	127.4	90.0	0.0	122.0	308	29	246	32	0.0	0.0	2.55E-07	0.0	0.0	0.0	4.08E-07	0.0	0.0	0.0	0.0	0.0	0.0	0.0	0.0	0.0	
47	30D	268	18	53	1	197	127.4	90.0	0.0	122.0	309	29	246	32	0.0	0.0	6.26E-07	0.0	0.0	0.0	6.26E-07	0.0	0.0	0.0	0.0	0.0	0.0	0.0	0.0	0.0	
47	30D	268	18	53	11	167	127.4	90.0	0.0	122.0	310	29	246	32	0.0	0.0	1.04E-06	0.0	0.0	0.0	1.04E-06	0.0	0.0	0.0	0.0	0.0	0.0	0.0	0.0	0.0	
47	30D	268	18	53	21	137	127.4	90.0	0.0	122.0	311	29	246	32	0.0	0.0	6.69E-07	0.0	0.0	0.0	6.69E-07	0.0	0.0	0.0	0.0	0.0	0.0	0.0	0.0	0.0	
47	30D	268	18	53	31	126	127.4	90.0	0.0	122.0	312	28	246	31	0.0	0.0	4.55E-07	0.0	0.0	0.0	2.75E-10	0.0	0.0	0.0	0.0	0.0	0.0	0.0	0.0	0.0	
47	30D	268	18	53	41	74	127.4	90.0	0.0	121.0	313	28	246	31	0.0	0.0	4.08E-07	0.0	0.0	0.0	4.08E-07	0.0	0.0	0.0	0.0	0.0	0.0	0.0	0.0	0.0	
47	30D	268	18	53	51	42	127.4	90.0	0.0	121.0	314	28	246	31	0.0	0.0	4.08E-07	0.0	0.0	0.0	4.08E-07	0.0	0.0	0.0	0.0	0.0	0.0	0.0	0.0	0.0	
47	31V	83	12	32	58	259	127.4	90.0	0.0	152.0	315	26	185	23	0.0	0.0	1.39E-10	0.0	0.0	0.0	1.39E-10	0.0	0.0	0.0	0.0	0.0	0.0	0.0	0.0	0.0	
47	31V	83	12	33	8	244	127.4	90.0	0.0	152.0	316	20	185	20	0.0	0.0	1.44E-10	0.0	0.0	0.0	1.44E-10	0.0	0.0	0.0	0.0	0.0	0.0	0.0	0.0	0.0	
47	31V	83	12	33	18	225	127.4	90.0	0.0	151.0	317	16	185	21	0.0	0.0	1.53E-10	0.0	0.0	0.0	1.53E-10	0.0	0.0	0.0	0.0	0.0	0.0	0.0	0.0	0.0	
47	31V	83	12	33	18	213	127.4	90.0	0.0	151.0	318	12	185	21	0.0	0.0	0.0	0.0	0.0	0.0	0.0	0.0	0.0	0.0	0.0	0.0	0.0	0.0	0.0		
47	31V	83	12	33	19	135	127.4	90.0	0.0	149.0	319	8	186	24	0.0	0.0	4.40E-10	0.0	0.0	0.0	4.40E-10	0.0	0.0	0.0	0.0	0.0	0.0	0.0	0.0	0.0	
47	31V	83	12	34	38	102	127.4	90.0	0.0	145.0	320	4	186	25	0.0	0.0	4.26E-10	0.0	0.0	0.0	4.26E-10	0.0	0.0	0.0	0.0	0.0	0.0	0.0	0.0	0.0	
47	31V	83	12	34	48	96	127.4	90.0	0.0	148.0	321	0	187	27	0.0	0.0	2.13E-10	0.0	0.0	0.0	2.13E-10	0.0	0.0	0.0	0.0	0.0	0.0	0.0	0.0	0.0	
47	31V	83	12	34	58	69	148.5	90.0	0.0	109.0	322	16	187	28	0.0	0.0	3.06E-09	0.0	0.0	0.0	3.06E-09	0.0	0.0	0.0	0.0	0.0	0.0	0.0	0.0	0.0	
47	31V	83	10	35	8	53	148.1	90.0	0.0	110.0	323	213	16	187	27	0.0	0.0	2.69E-09	0.0	0.0	0.0	2.69E-09	0.0	0.0	0.0	0.0	0.0	0.0	0.0	0.0	0.0
47	31V	83	10	35	18	36	147.7	90.0	0.0	110.0	324	213	15	187	27	0.0	0.0	1.50E-09	0.0	0.0	0.0	1.50E-09	0.0	0.0	0.0	0.0	0.0	0.0	0.0	0.0	0.0
47	31V	83	10	35	28	20	147.3	90.0	0.0	111.0	325	214	17	187	28	0.0	0.0	7.18E-10	0.0	0.0	0.0	7.18E-10	0.0	0.0	0.0	0.0	0.0	0.0	0.0	0.0	0.0
47	31V	83	10	35	38	3	147.0	90.0	0.0	111.0	326	214	17	187	28	0.0	0.0	5.88E-10	0.0	0.0	0.0	5.88E-10	0.0	0.0	0.0	0.0	0.0	0.0	0.0	0.0	0.0
47	31V	83	10	35	48	0	146.5	72.0	0.0	104.0	327	224	23	211	31	0.0	0.0	4.58E-10	0.0	0.0	0.0	4.58E-10	0.0	0.0	0.0	0.0	0.0	0.0	0.0	0.0	0.0

RUN	D	GET	TAN	SUM	OBS	SCAT	OAG	CBS	ANG	LON	LAT	125CA	136Cf	150DA	192CA	2380A	2469A	290CA	290C
NJ.	N	DAY	F	S	ALT	ANG	LON	LAT	F6.1	14	14	14	14	1PE9.2	1PE9.2	1PE9.2	1PE9.2	1PE9.2	
14	A2	14	13	13	13	13	13	13	F6.1										
34N	82	15	35	15	129	143.9	90.7	108.4	135	16	111	25	0.0	0.0	0.0	0.0	0.0	0.0	
34N	83	15	35	25	113	148.5	90.5	109.3	136	16	112	26	0.0	0.0	0.0	0.0	0.0	0.0	
34N	83	15	35	35	37	148.1	90.0	109.8	136	17	112	27	0.0	0.0	0.0	0.0	0.0	0.0	
34N	83	15	35	55	31	147.8	90.0	110.3	137	17	112	27	0.0	0.0	0.0	0.0	0.0	0.0	
34N	83	15	35	55	64	147.4	90.0	110.3	137	17	112	27	0.0	0.0	0.0	0.0	0.0	0.0	
34N	93	15	36	5	43	147.0	90.0	111.4	139	18	112	28	0.0	0.0	0.0	0.0	0.0	0.0	
34N	93	15	36	15	31	146.6	90.0	111.9	138	18	112	28	0.0	0.0	0.0	0.0	0.0	0.0	
34N	93	15	36	25	15	145.2	90.0	112.4	139	18	113	29	0.0	0.0	0.0	0.0	0.0	0.0	
34N	93	15	36	35	5	146.9	90.0	111.6	139	18	114	29	0.0	0.0	0.0	0.0	0.0	0.0	
34N	93	15	39	35	2	145.6	72.4	125.4	149	24	136	32	0.0	0.0	0.0	0.0	0.0	0.0	
34N	83	15	42	35	2	136.0	65.7	109.1	159	28	15C	36	0.0	0.0	0.0	0.0	0.0	0.0	
35N	93	17	13	56	279	151.4	95.0	104.1	136	13	85	20	0.0	0.0	0.0	0.0	0.0	0.0	
35N	93	17	14	6	254	151.5	90.0	124.6	136	13	85	21	0.0	0.0	0.0	0.0	0.0	0.0	
35N	93	17	14	16	243	151.2	90.0	105.2	107	14	85	21	0.0	0.0	0.0	0.0	0.0	0.0	
35N	83	17	14	25	233	150.9	90.0	105.5	107	14	85	22	0.0	0.0	0.0	0.0	0.0	0.0	
35N	93	17	14	36	217	150.6	90.0	126.2	128	14	85	23	0.0	0.0	0.0	0.0	0.0	0.0	
35N	83	17	14	46	202	150.3	90.0	106.5	109	15	86	23	0.0	0.0	0.0	0.0	0.0	0.0	
35N	83	17	14	56	135	150.0	90.0	107.0	109	15	86	24	0.0	0.0	0.0	0.0	0.0	0.0	
35N	83	17	15	6	172	149.5	90.0	137.8	109	15	86	24	0.0	0.0	0.0	0.0	0.0	0.0	
35N	93	17	15	16	155	149.1	90.0	108.3	110	16	86	25	0.0	0.0	0.0	0.0	0.0	0.0	
35N	93	17	15	26	142	148.4	90.0	128.8	110	16	86	25	0.0	0.0	0.0	0.0	0.0	0.0	
35N	83	17	15	36	124	148.4	90.0	129.3	111	16	86	26	0.0	0.0	0.0	0.0	0.0	0.0	
35N	93	17	15	46	129	148.1	90.0	129.8	111	17	87	27	0.0	0.0	0.0	0.0	0.0	0.0	
35N	83	17	15	56	92	147.7	92.0	110.4	112	17	87	27	0.0	0.0	0.0	0.0	0.0	0.0	
35N	93	17	16	6	75	147.3	90.0	110.9	112	17	87	28	0.0	0.0	0.0	0.0	0.0	0.0	
35N	93	17	16	59	147.0	90.0	111.4	113	18	87	29	0.0	0.0	0.0	0.0	0.0	0.0		
35N	93	17	16	26	43	146.6	90.0	111.9	113	18	87	29	0.0	0.0	0.0	0.0	0.0	0.0	
35N	83	17	16	35	26	146.2	90.0	112.4	114	18	87	29	0.0	0.0	0.0	0.0	0.0	0.0	
35N	93	17	16	46	12	145.8	90.0	112.9	114	19	88	30	0.0	0.0	0.0	0.0	0.0	0.0	
35N	93	17	16	56	3	147.2	97.0	111.0	115	19	91	30	0.0	0.0	0.0	0.0	0.0	0.0	
35N	83	17	19	56	3	145.1	72.2	125.8	124	24	111	32	0.0	0.0	0.0	0.0	0.0	0.0	
36D	225	C	19	57	233	28.7	65.6	109.6	134	28	126	37	0.0	0.0	0.0	0.0	0.0	0.0	
36D	225	C	19	57	233	28.7	90.0	109.6	224	34	206	19	0.0	0.0	0.0	0.0	0.0	0.0	
36D	225	C	19	57	77	29.0	90.0	112.0	114	19	88	30	0.0	0.0	0.0	0.0	0.0	0.0	
36D	225	C	19	57	52	3C.5	90.0	111.0	99	225	35	207	19	0.0	0.0	0.0	0.0	0.0	
36D	225	C	19	57	23	30.8	90.0	112.3	226	35	207	18	0.0	0.0	0.0	0.0	0.0	0.0	
36D	225	C	19	57	137	29.7	90.0	110.3	227	35	207	18	0.0	0.0	0.0	0.0	0.0	0.0	
36D	225	C	19	47	134	3C.C	90.0	111.2	228	35	207	18	0.0	0.0	0.0	0.0	0.0	0.0	
36D	225	C	19	57	77	30.3	90.0	111.6	229	35	208	17	0.0	0.0	0.0	0.0	0.0	0.0	
36D	225	C	19	57	52	29.6	77.9	90.0	125.4	172	34	155	20	0.0	0.0	0.0	0.0	0.0	
36D	225	C	20	57	2	3C.5	90.0	108.9	173	34	156	19	0.0	0.0	0.0	0.0	0.0	0.0	
36D	225	C	20	57	23	30.8	90.0	112.3	230	35	208	17	0.0	0.0	0.0	0.0	0.0	0.0	
36D	225	C	20	57	3	32.6	87.8	114.6	231	35	210	18	0.0	0.0	0.0	0.0	0.0	0.0	
37D	225	C	19	57	2	35.5	94.0	118.1	231	35	213	21	0.0	0.0	0.0	0.0	0.0	0.0	
37D	225	C	19	57	296	27.9	90.0	125.4	172	34	155	20	0.0	0.0	0.0	0.0	0.0	0.0	
37D	225	C	19	57	52	28.3	90.0	108.9	173	34	156	19	0.0	0.0	0.0	0.0	0.0	0.0	
37D	225	C	19	57	23	30.8	90.0	111.0	229	35	208	17	0.0	0.0	0.0	0.0	0.0	0.0	
37D	225	C	19	57	27	3	32.6	87.8	114.6	231	35	210	18	0.0	0.0	0.0	0.0	0.0	
37D	225	C	19	57	3	35.5	94.0	118.1	231	35	213	21	0.0	0.0	0.0	0.0	0.0	0.0	
37D	225	C	19	57	2	38.5	94.0	118.1	231	35	214	21	0.0	0.0	0.0	0.0	0.0	0.0	
37D	225	C	19	57	23	28.3	90.0	108.9	173	34	156	19	0.0	0.0	0.0	0.0	0.0	0.0	
37D	225	C	19	57	23	30.8	90.0	112.3	230	35	208	17	0.0	0.0	0.0	0.0	0.0	0.0	
37D	225	C	19	57	3	32.6	87.8	114.6	231	35	210	18	0.0	0.0	0.0	0.0	0.0	0.0	
37D	225	C	19	57	2	35.5	94.0	118.1	231	35	213	21	0.0	0.0	0.0	0.0	0.0	0.0	
37D	225	C	19	57	2	38.5	94.0	118.1	231	35	214	21	0.0	0.0	0.0	0.0	0.0	0.0	
37D	225	C	19	57	2	39.3	177	29.1	90.0	110.1	176	35	156	18	0.0	0.0	0.0	0.0	
37D	225	C	19	57	152	25.3	90.0	110.4	176	35	157	18	0.0	0.0	0.0	0.0	0.0	0.0	

DATA ANALYSIS

A major problem in comparing various airglow measurements is that of reducing the results to some common basis by eliminating the angular dependence of the measurements. The angles on which these measurements depend are the solar zenith angle, θ , and the line of sight zenith angle, ψ . The common basis usually chosen for comparison is the case in which both of these angles are zero. It was shown in Eq. (5) that the total received radiation is given by

$$I_T = \alpha \int_{s=0}^{\infty} I(s) T(s) ds \quad (5)$$

According to Beer's law, the atmospheric transmission, $T(s)$, can be expressed as

$$T(s) = \exp \left[- \sum_i \sigma_i N_i(s) \right] \quad (7)$$

where

σ_i = absorption cross section of the i^{th} atmospheric constituent

$N_i(s)$ = total number of particles per unit area of the i^{th} constituent between the point s and the detector

By definition,

$$N_i(s) = \int_{t=s}^{\infty} n_i(t) dt \quad (8)$$

where $n_i(t)$ is the number density of the i^{th} constituent along the line of sight vector.

Since most atmospheric quantities are expressed as functions of altitude along the local vertical, we make the transformation

$$ds = dy \sec \varphi_y \quad (9)$$

where φ_y is the angle between the line of sight and the local vertical at an altitude of y kilometers. The total received radiation is given by

$$I_T = \alpha \int_{y=0}^{\infty} I(y) \exp \left[- \sum_i \sigma_i \int_{t=y}^{\infty} n_i(t) \sec \varphi_t dt \right] \sec \varphi_y dy \quad (10)$$

From Fig. 8 it can be seen that

$$\sec \varphi_y = \left[1 - \left(\frac{R_e}{R_e + y} \right)^2 \sin^2 \varphi_o \right]^{-\frac{1}{2}} \quad (11)$$

When the line of sight does not intersect the earth, the $s = 0$ location is taken to be the tangent altitude point. This point indicates where the line of sight vector makes its closest approach to the earth. In this case, the total received radiation can be expressed as

$$I_T = \int_{y_h}^{\infty} [\cdot] T(y, \infty) dy + \int_{y_h}^{\infty} [\cdot] [T'(y_h, y) + T'(y_h, \infty)] dy \quad (12)$$

where

$$[\cdot] = \alpha I(y) \sec \varphi_y$$

y_h = tangent altitude

$T'(a, b)$ = transmission of solar energy from point a to point b

and $T'(A, b)$ has the same definition except that φ_t is always greater than 90 degrees.

In the expressions given above, $I(y)$ is the volume emission rate of the atmosphere at the height y . This volume emission rate can be produced by several phenomena. For the analysis of our data, however, we believe that only two sources of radiation are important — Rayleigh scattering and photoelectron excitation.

For a Rayleigh scattering atmosphere, the theory is well known (Ref. 6) and we have

$$I(y, \lambda) = \frac{3}{16\pi} k_s (1 + \cos^2 \psi) \rho(y) H(\lambda) T(y, \theta_y) \quad (13)$$

where

- k_s = Rayleigh scattering coefficient (cm^{-1})
- ψ = Rayleigh scattering angle
- θ_y = angle between the sun line and the local vertical at the altitude y
- $\rho(y)$ = total atmospheric number density at an altitude $h(\text{cm}^{-3})$
- $H(\lambda)$ = solar irradiance at the top of the atmosphere at the wavelength $\lambda(\text{w/cm}^2)$
- $T(y, \theta_y)$ = transmission of the solar energy from the top of the atmosphere to the altitude y

The term $H(\lambda)T(y, \theta_y)$ is the amount of solar energy of wavelength λ that reaches an altitude y along the slant path described by θ_y . The other term, $\frac{3}{16\pi} k_s (1 + \cos^2 \psi) \rho(y)$, describes how much of this transmitted energy is electromagnetically scattered along the line of sight vector.

When the radiation is the result of photoelectron excitation, the volume emission rate is theoretically given by (Refs. 9,10)

$$I(y, \lambda) = \sum_l \sum_j \beta_{kj} r_j f_j \quad (14)$$

where

k = the electronic state from which the transition to the ground state produces radiation of wavelength λ

β_{kj} = branching ratio or probability of a transition from the state j to the state k

f_j = the fraction of depopulations of the state j that produces radiation

$r_{j\ell}(y, \theta)$ = the rate of population of the j^{th} state of the ℓ^{th} species

The rate of population of the j^{th} state is proportional to the amount of energy lost during a collision with a photoelectron of energy E_p , and, therefore, is also proportional to the number of such photoelectrons produced by solar ionization. Thus, we have

$$r_{j\ell} = \int_{E_p > E_j} Q_p \times E_{j\ell} \quad (15)$$

where

$Q_p(y, \theta)$ = production rate of photoelectrons with energy E_p

$E_{j\ell}$ = energy deposited in the j^{th} state through a collision with an electron of energy E_p

The production rate of photoelectrons can be given as

$$Q_p(y, \theta) = \sum_{i \ell} \sigma_{i\ell}(\lambda_p) n_\ell(y) H(\lambda_p) \exp \left[- \sum_m \sigma_m \int_y^\infty n_m(t) \sec \theta t dt \right] \quad (16)$$

where

σ_{il} = cross section for the i^{th} ionization state of the l^{th} species

n_l = particle density of the l^{th} species

Obviously this relationship is complicated and many of the variables, such as the absorption and collision cross sections, are not known precisely. A complete investigation at this level is beyond the scope of this study. From the limb measurements, we have found that the emission rate follows an altitude profile with a peak near 175 kilometers. Therefore, $I(y)$ can be approximated by a general distribution function of the form

$$I(y) = I_p \frac{(1 + a^2)e^{(y-y_p)/h}}{(a + e^{(y-y_p)/h})^2} \quad (17)$$

The parameters a , h , y_p and I_p must be adjusted so that the predicted irradiance matches the measured values.

The practical application of the theories given above can only be accomplished with the assistance of high speed electronic computers. For this reason, several computer programs were devised in 1970 to allow us adequate flexibility in the data analysis. In these computer programs, we only consider atmospheric absorption by ozone and molecular oxygen. Table 6 gives the parameters for the various distributions (concentrations versus altitude, etc.) used in the programs. These distributions represent a 600°K model atmosphere that matched the density measurements obtained by Hayes and Robles (Ref. 16) using the WEP. The values of the absorption coefficients and the solar flux used in the programs were obtained from published data (Refs. 12,13,16). All wavelength dependent parameters are averaged over 50^{A} intervals. The spectral shapes of the WEP are also incorporated into the program.

Using the WEP filter curves, the expected outputs of the photometers are calculated by averaging over the effective half bandwidths of the filters. Thus, if $S_{ij}(\lambda)$ is the filter shape of the j^{th} filter on photometer i , then

Table 6

DISTRIBUTION PARAMETERSGeneral Distribution Function

$$x(y) = \frac{(1+a)e^{(y-y_p)/h_a}}{(a+e^{(y-y_p)/h_a})^2}$$

DistributionsLBH Radiation

$$a = 1.0$$

$$y_p = 175 \text{ km}$$

$$h = 25 \text{ km}$$

O₂ Density

$$y < 163 \text{ km}$$

$$a = .3594$$

$$y_p = 0$$

$$h = -5.9 \text{ km}$$

$$y > 163 \text{ km}$$

$$a = - .9999469$$

$$y_p = 0$$

$$h = - 31$$

O₃ Density

$$a = 0$$

$$y_p = 23.5 \text{ km}$$

$$h = - 4.63$$

$$y < 23.5 \text{ km}$$

$$+ 4.63$$

$$y > 23.5 \text{ km}$$

Total Atmosphere

$$y < 150 \text{ km}$$

$$a = 5.0$$

$$y_p = 0$$

$$h = - 7.057$$

$$y > 150 \text{ km}$$

$$a = - .99992$$

$$y_p = 0$$

$$h = - 62.04$$

$$I_{ij} = \frac{1}{B_{ij}} \int_{\lambda=0}^{\infty} S_{ij}(\lambda) I_T(\lambda) d\lambda \quad (18)$$

$$= \frac{1}{B_{ij}} \left[50\text{\AA} \times \sum_k S_{ij}(\Delta_k + 1000\text{\AA}) I_T(\Delta_k + 1000\text{\AA}) \right] \quad (19)$$

where

B_{ij} = the effective half bandwidth of the j^{th} filter of photometer i

Δ_k = 50\AA intervals

The inputs to this particular program are the tangent altitude and the three angles ϕ_o (line of sight zenith angle), θ_o (sun zenith angle), and ψ (scattering angle) all measured at the earth's surface or at the tangent altitude point. These quantities are provided by another Grumman program that gives a complete analysis of the OAO viewing geometry during the observation periods. The output of the program is the expected irradiance at 50\AA intervals produced by both Rayleigh scattering and photoelectron excitation. Also given are the irradiance values expected to be obtained from the WEP filter photometers.

For each measurement sequence, a series of theoretical irradiance values was calculated. Parameters in the program were then varied until the theoretically predicted sequence matched the measured values. The irradiance was then calculated using these parameters for the case when both the viewing and the solar zenith angles were zero. This zero-zero case is used to compare the results of other experimenters.

The variation of the received radiation as the viewing area scans across the earth during a typical measurement sequence is shown in Figs. 5-7. In each of these sequences, the OAO field of view initially moves across the dark earth onto the sunlit earth and then through the sunlit limb and onto the star. The radiation increases rather sharply as the viewing moves across the sunlit earth. This is the result of the particular viewing geometry

associated with all these observations. During this portion of the scan, the solar zenith angle, θ , was decreasing and the line of sight zenith angle, φ , was increasing as shown in Fig. 9. The first effect means that less solar radiation is absorbed by higher altitude constituents. The second effect results in measurements of greater amounts of sunlit atmosphere as the viewing moves across the earth. Measurements during this same sequence of the dayglow in the 1920\AA region are shown in Fig. 6. Notice that these measurements do not show the sharp maximum in received radiation.

These measurements have been reduced to the case when both the sun and the line of sight lie along the local zenith ($\theta = 0^\circ$, $\varphi = 0^\circ$). This provides a common basis from which the WEP measurements can be compared to theoretical predictions and results of other experiments. The radiances for this case, averaged over five orbits, are plotted in Fig. 10 for each filter. Also shown are the radiance values predicted by the Rayleigh scattering calculation. Note that only the values in the vacuum ultraviolet are shown since the dayglow saturated all WEP photometers using filters above 2000\AA . Figure 10 shows that the only measurements that agree with the Rayleigh scattering prediction are those in the 1920\AA spectral band. These measurements also agree with the results of Barth and Mackey (Ref. 1) and Elliott et al. (Ref. 17).

The spectral region covered by the 1500\AA photometer is of particular interest. The measurements in this region agree with the data from the NRL experiment on OGO-4 and clearly indicate that the very low estimate of the earth's radiance predicted by Rayleigh scattering does not exist. The high level of radiation in the 1500\AA region is believed to be the result of electronic excitation of molecular nitrogen by high energy photoelectrons ($> 7 \text{ eV}$). These photoelectrons are produced from the ionization of high altitude atmospheric constituents by the extreme ultraviolet solar radiation. The principal emissions are from the Lyman-Birge-Hopfield ($a' \pi_g - x' \Sigma_g^+$), Birge Hopfield ($b' \pi_u - x' \Sigma_g^+$) and Vegard-Kaplan ($A^3 \Sigma_u^+ - x' \Sigma_g^+$) bands of molecular nitrogen. These transitions produce radiation in the 1350 to 1800\AA spectral region. This mechanism was first considered theoretically by Barth and Green (Ref. 9) and later by Dalgarno et al. (Ref. 10). Prinz and Meier (Ref. 11) of NRL have used some of the more recent measurements of ionization cross sections, photoelectron collision cross sections, and quenching coefficients in determining the expected emissions from this mechanism. Their calculation

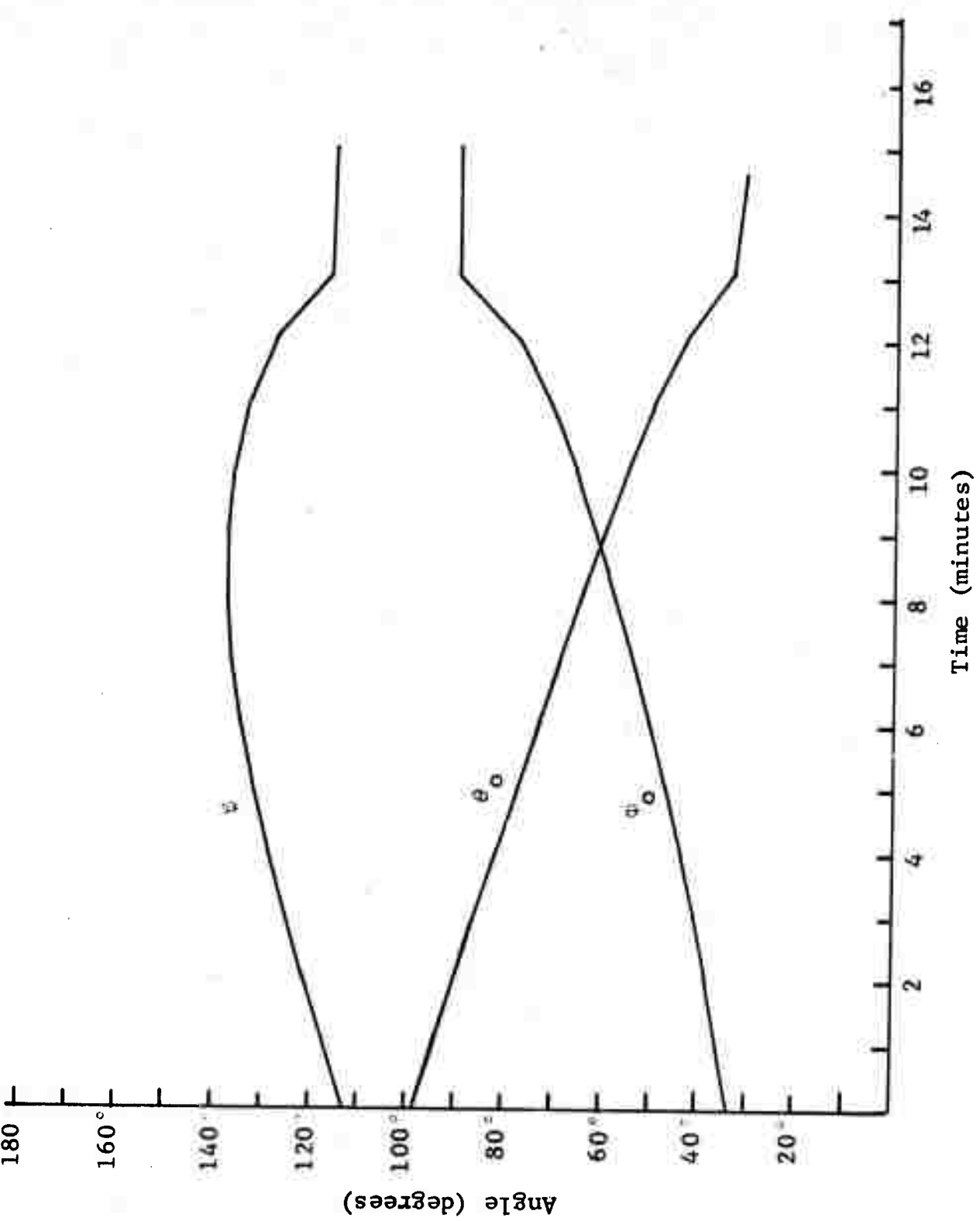


Fig. 9 Variation of Angles for Orbit 7903

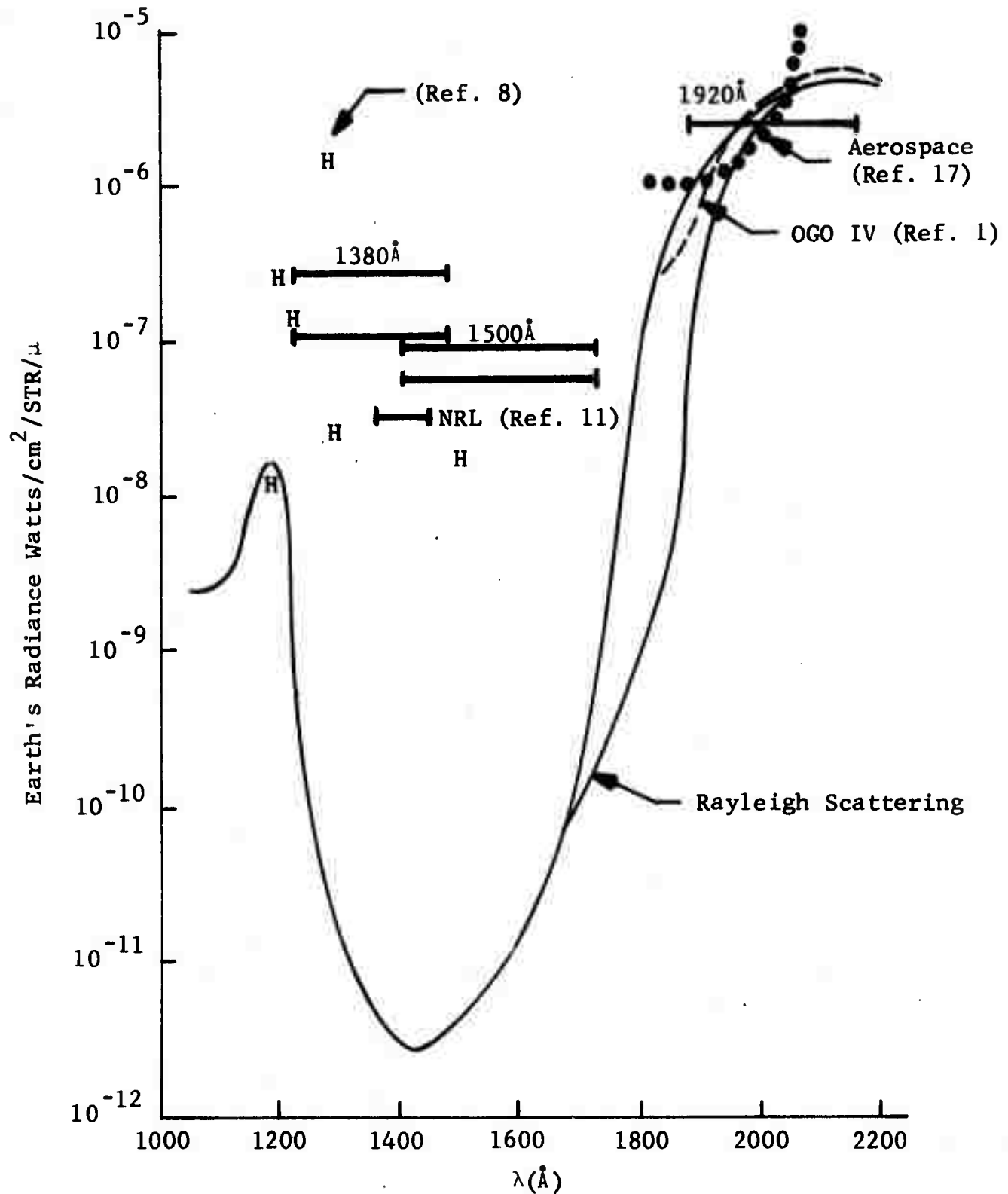


Fig. 10 Comparison of OAO Measurements with Other Experimental Measurements. Values are for 1380 Å, 1500 Å, and 1920 Å Filters. Lower line represents the measured value minus the expected contribution of the 1304 Å oxygen line.

predicts that the columnar emission rate from this system should be 6.5 kR or $3.3 \times 10^{-8} \text{ w/cm}^2\text{-ster}\cdot\mu$ between 1350 and 1800\AA . They also indicate that a peak in the emission rate should exist near 180 kilometers.

Detailed measurements of the sunlit limb with the 1500\AA filter and using the half second sampling mode of the WEP, are shown in Fig. 11. These measurements show a sharp peak in the received radiation near a tangent altitude of 175 kilometers. Because of the small field of view of the WEP photometers, it is reasonable to assume that the volume emission rate also has a maximum near 175 kilometers. The gaps in measurements, as shown in Fig. 11, are due to the delay in the issuance of new exposure commands. It should be noted that part of the radiation measured by the 1500\AA filter is due to the emission from the 1304\AA triplet of atomic oxygen. Assuming that the strength of this line is approximately $4 \times 10^{-9} \text{ w/cm}^2\text{-ster}$ as measured by Barth and Schaffner (Ref. 2), then this represents only 4 percent of the measured energy. Because of the near zero transmission of the 1500\AA filter at 1200\AA , the Lyman alpha emission of atomic hydrogen also does not contribute to radiation measured by this filter. Therefore, the only radiation of significance is that produced by the LBH bands of N_2 . The variation of the 1500\AA radiation with tangent altitude is shown in Figs. 12-14. It also should be noted that the radiance value given in Fig. 10 for the 1500\AA measurements is an approximate value since the model chosen for the nitrogen emissions did not include the effects of the solar angle.

The measurements with the 1920\AA filter, as mentioned, agree very well with values predicted by the Rayleigh scattering model. Results of the measurements of the sunlit limb using this filter are shown in Fig. 15. It can be seen that no large peak in the received radiation occurs as a function of tangent altitude in this wavelength region.

The radiation measured by the 1250\AA filter is almost entirely due to the Lyman alpha emissions of atomic hydrogen at 1216\AA . Part of the radiation can be attributed to the 1304 and 1356\AA lines of atomic OI and also to the 1358\AA LBH band of N_2 . Although no detailed measurements, using half second sampling, of the sunlit limb were made at 1250\AA , a good picture of the limb was obtained with the Mode C measurements. As shown in Fig. 16, the 1250\AA radiation also shows a peak in the received radiation near 175 kilometers. It should be noted that radiation in this spectral region is very dependent on solar activity, explaining the spread in measured values.

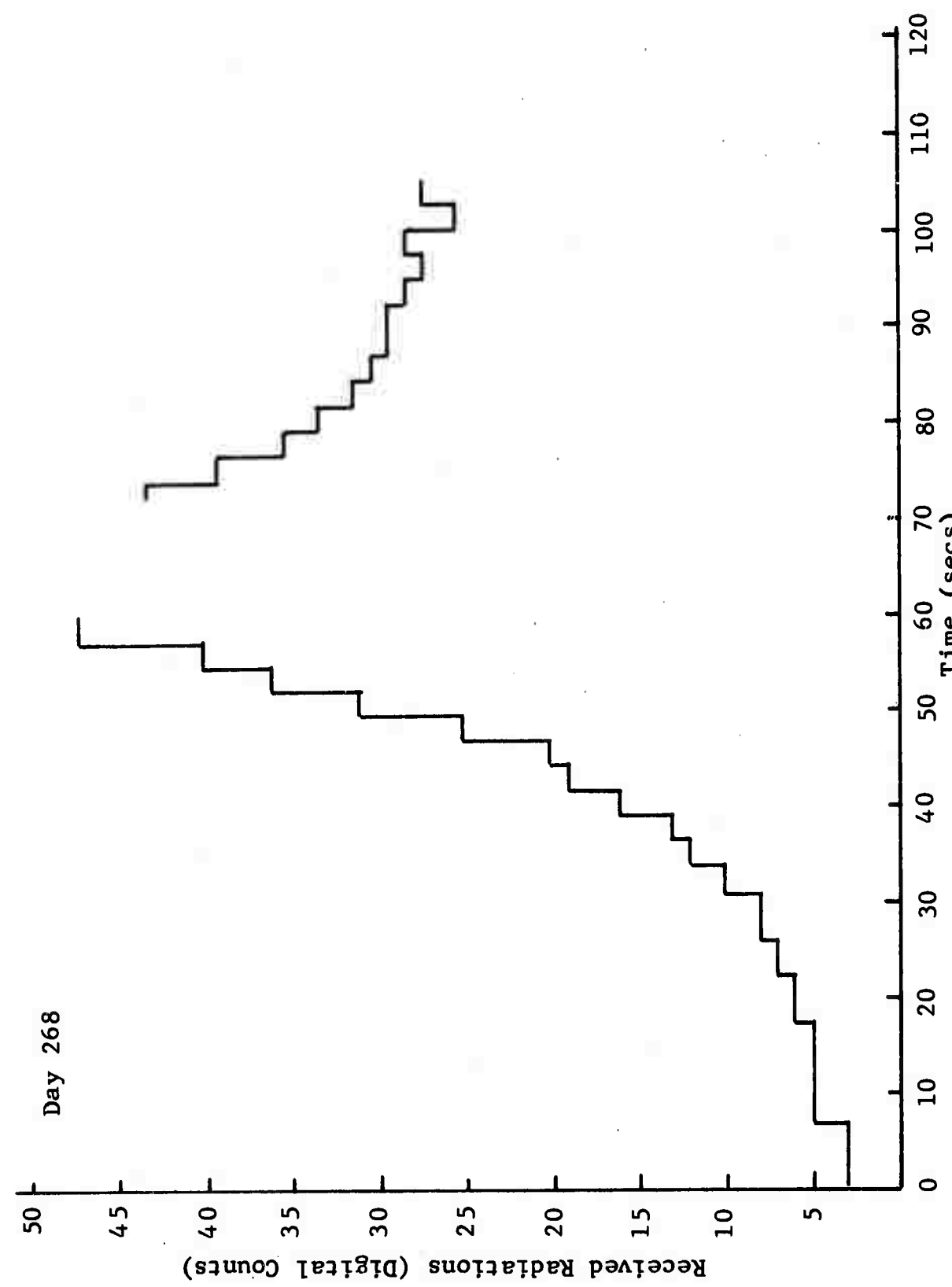


Fig. 11 1500 Å Limb Measurement

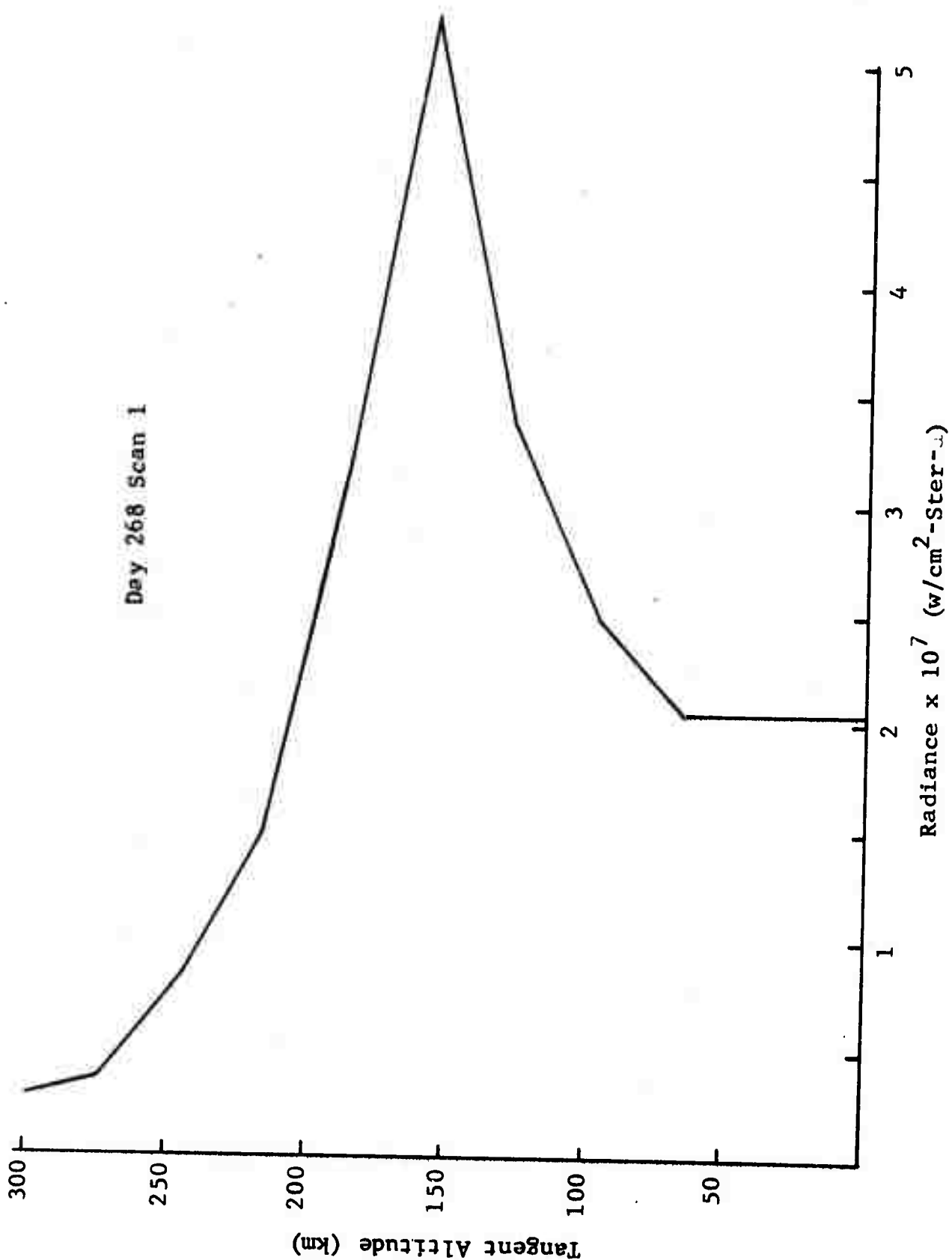


Fig. 12 Altitude Profile of 1500 Å Radiation

Day 268 Scan 2

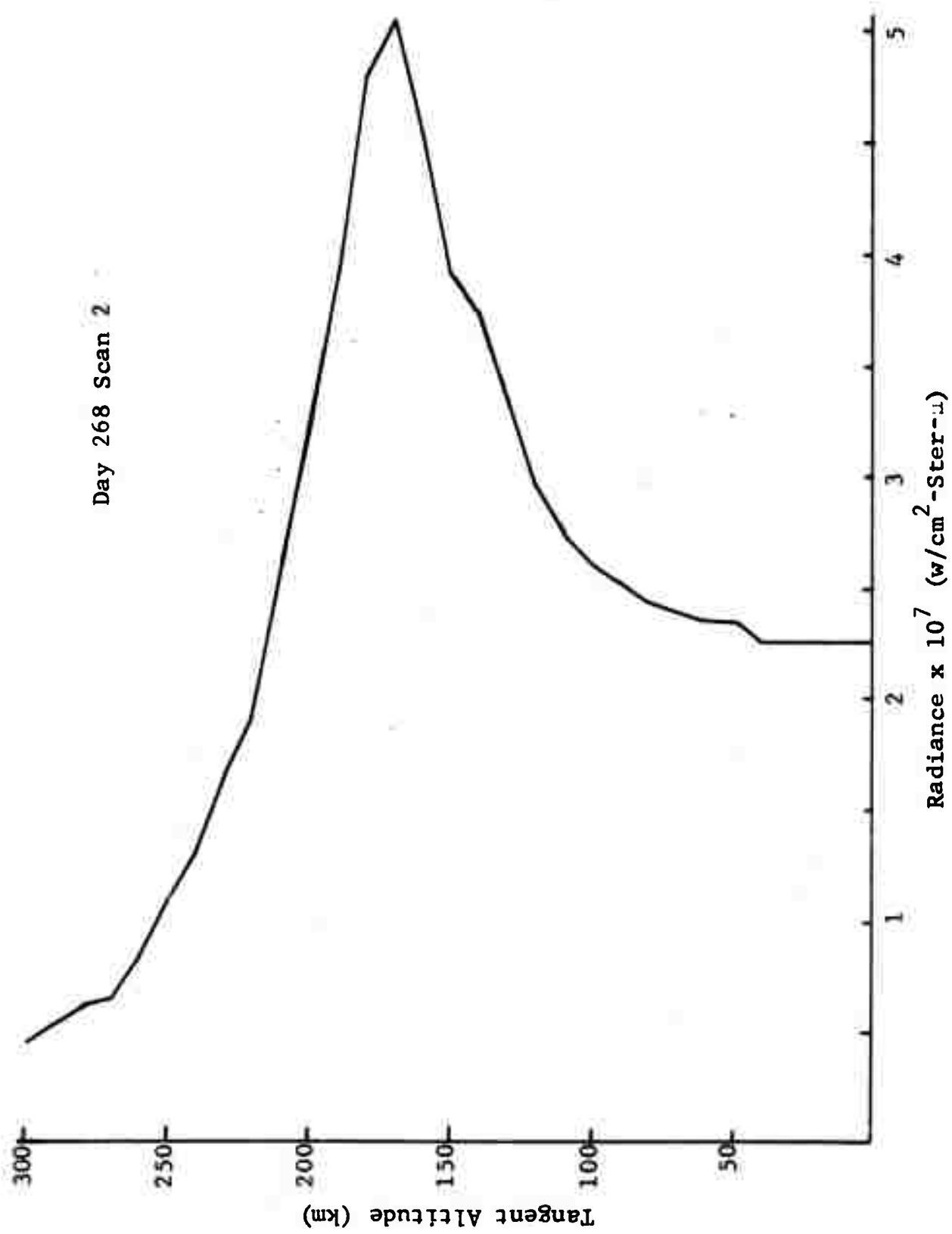


Fig. 13 Altitude Profile of 1500 Å Radiation

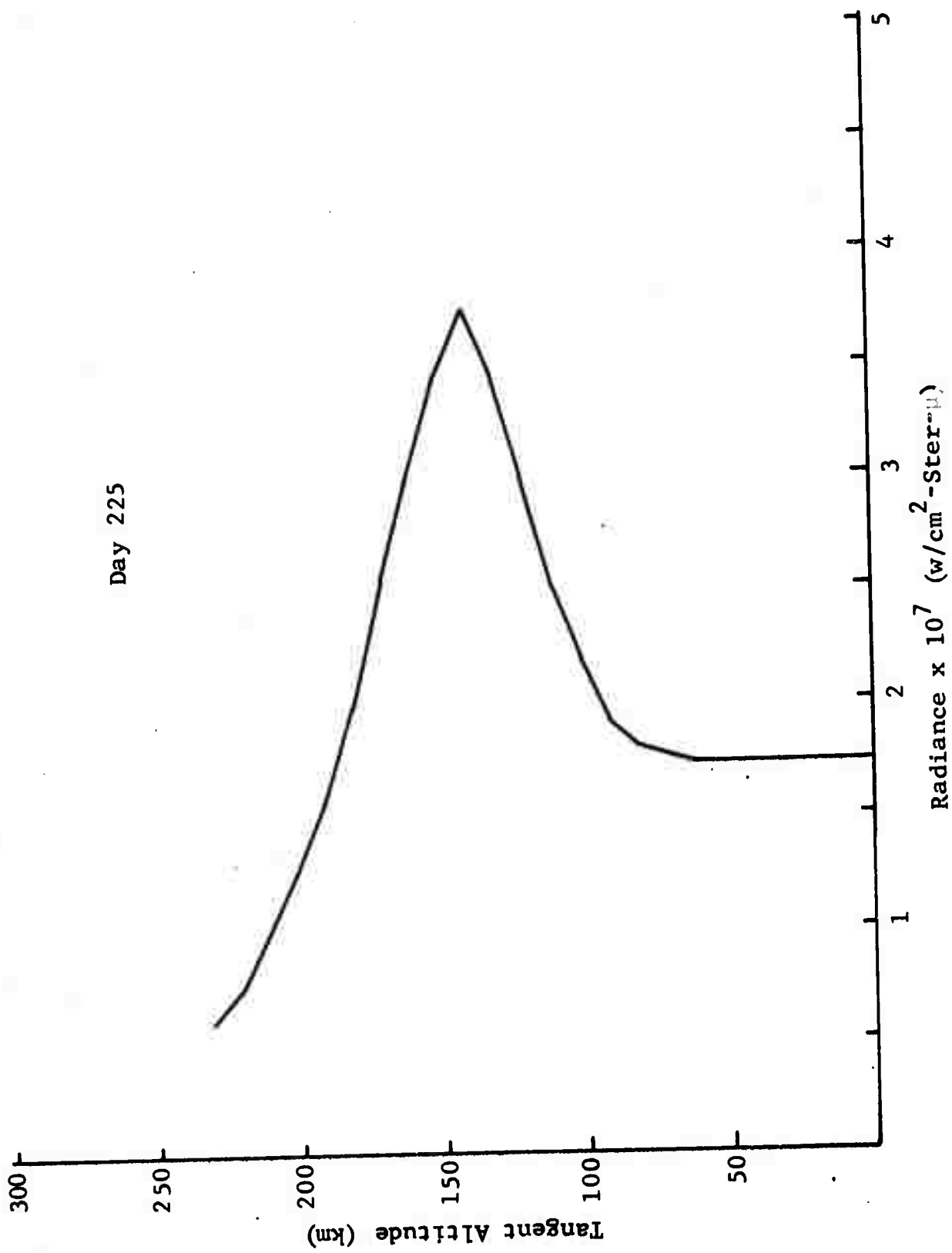


Fig. 14 Altitude Profile of 1500\AA Radiation

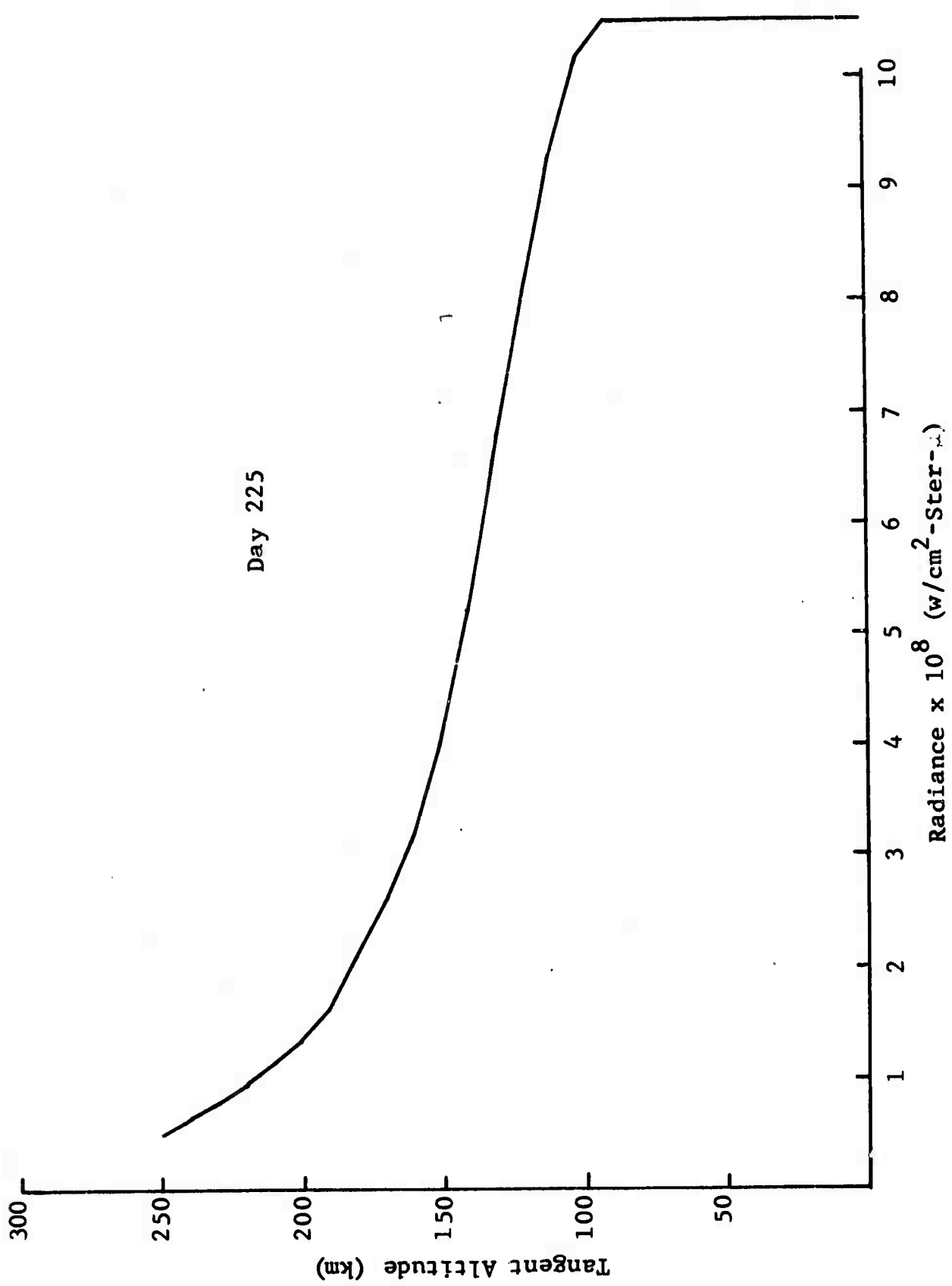


Fig. 15 Altitude Profile of 1920A Radiation

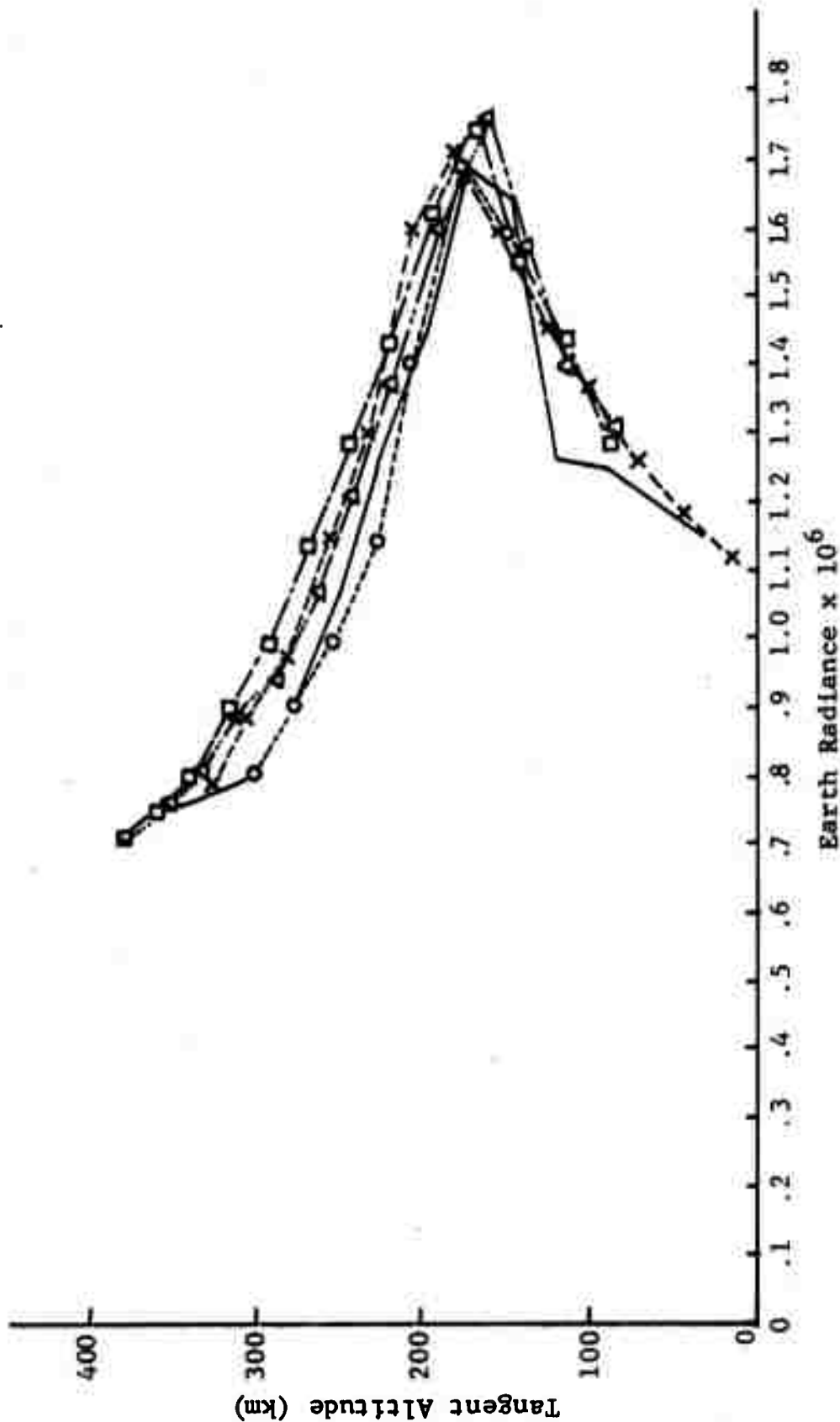


Fig. 16 Altitude Profile of 1250 \AA Radiation

The vacuum ultraviolet nightglow is barely a measurable feature. The measurements, using the 1250 \AA filter, show the radiance to be independent of altitude with a magnitude of about $10^{-8} \text{ w/cm}^2 \text{ ster-}\mu$, which is slightly above the noise level of the photometer. The source of this radiation was postulated by Meier (Ref. 4) to be scattered Lyman alpha emission from the sunlit portions of the upper atmosphere. The output from the 1500 \AA filter was at the noise level of the photometer for all nightglow measurements. This noise level is equivalent to an irradiance of $4.8 \times 10^{-14} \text{ w/cm}^2\text{-}\mu$. In the 1920 \AA region, the nightglow was measurable. The limb measurements showed a distinct altitude profile to the emission, as is shown in Fig. 17, with a peak in the received radiation occurring at a tangent altitude of about 70 kilometers. A similar spike in the nightglow was measured by Stecher (Ref. 15) at 1800 \AA . At present, the source of this radiation has not been identified. The prominent features of the ultraviolet nightglow occurred in the spectral region measured by the 2380 and 2980 \AA filters. The emissions measured by the 2980 \AA filter show a sharp peak occurring near 110 kilometers (Fig. 18). This maximum was also observed by Stecher (Ref. 15) and later by Hennes (Ref. 14). Their rocket spectrometers show the peak occurring near 97 kilometers. The spectrum obtained by both experiments indicate that the source of the radiation are the Herzberg bands of molecular oxygen. This band system produces emissions between 2500 and 3500 \AA . The most prominent feature of the spectrum is the large maximum near 3000 \AA produced by the Herzberg (7,4) and (5,3) bands at 2976 and 2945 \AA and by the 2972 \AA line of atomic oxygen. Figure 19 shows the altitude profile of the received radiation from the 2380 \AA filter and Fig. 20 shows the radiation measured by the 2460 \AA filter. These measurements also show a peak near 110 kilometers and, therefore, are probably measuring some of the lower wavelength bands of the Herzberg system.

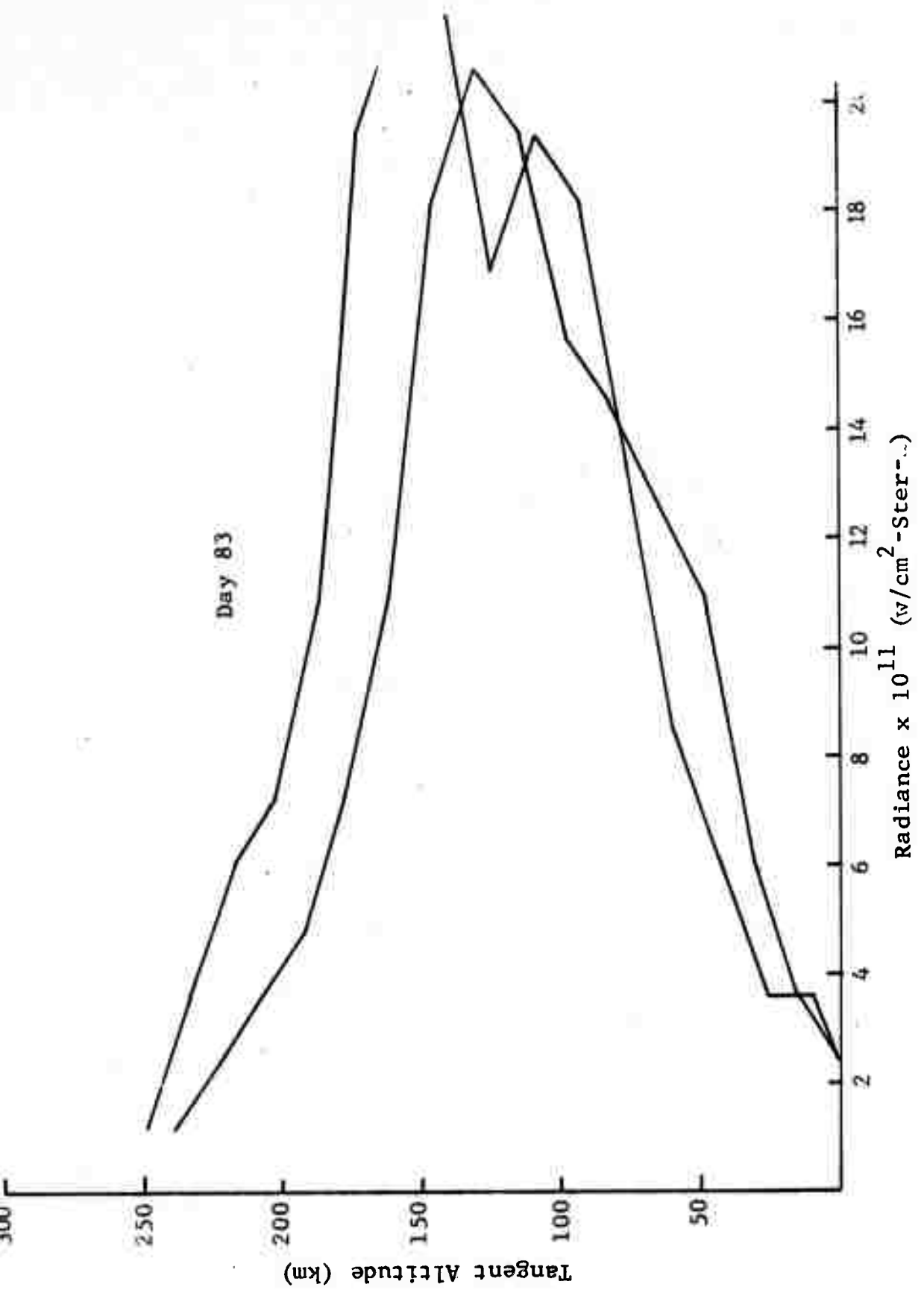


Fig. 17 Altitude Profile of the 1920 Å Nightglow

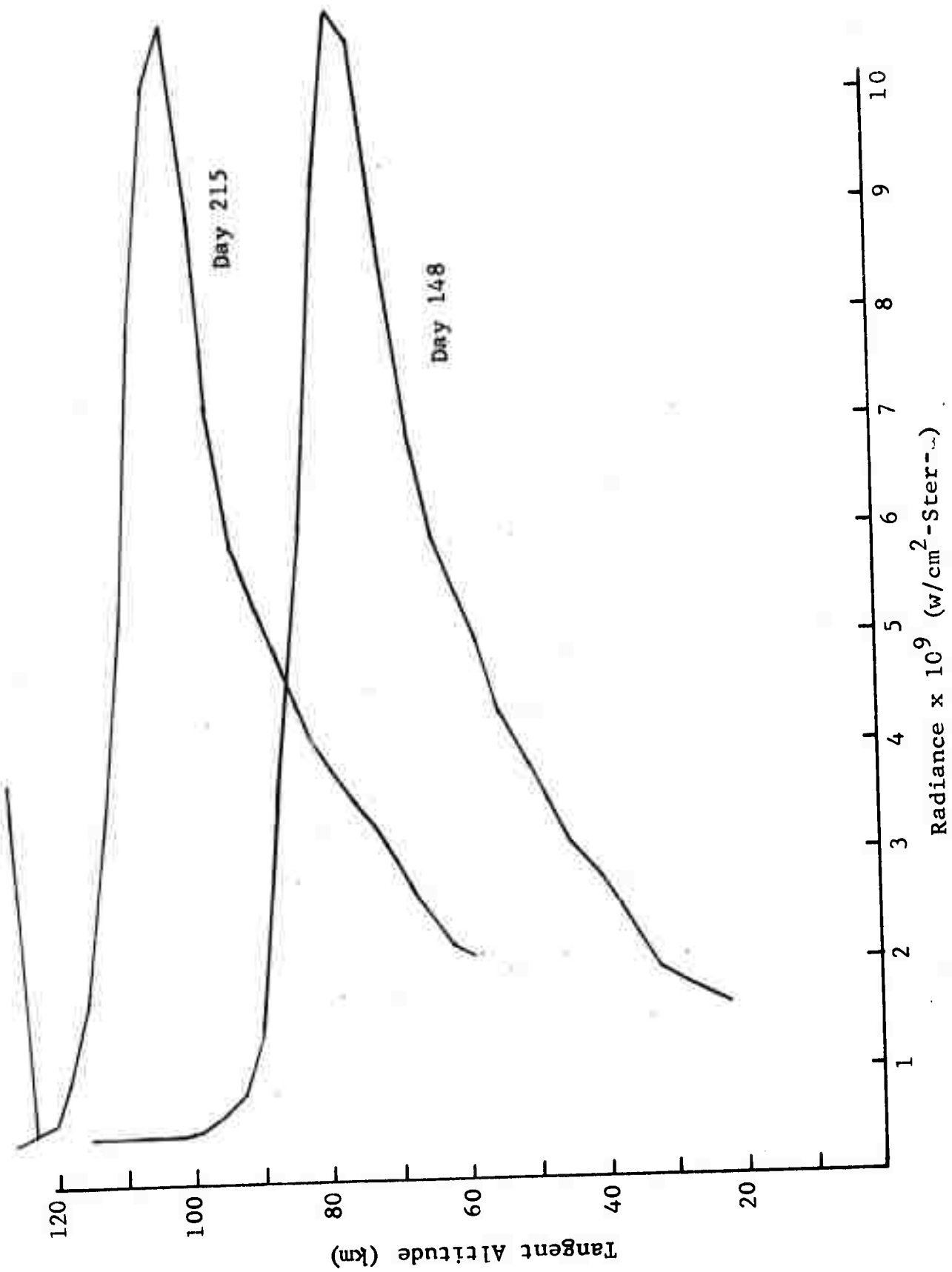


Fig. 18 Altitude Profile of the 2980 Å Nightglow

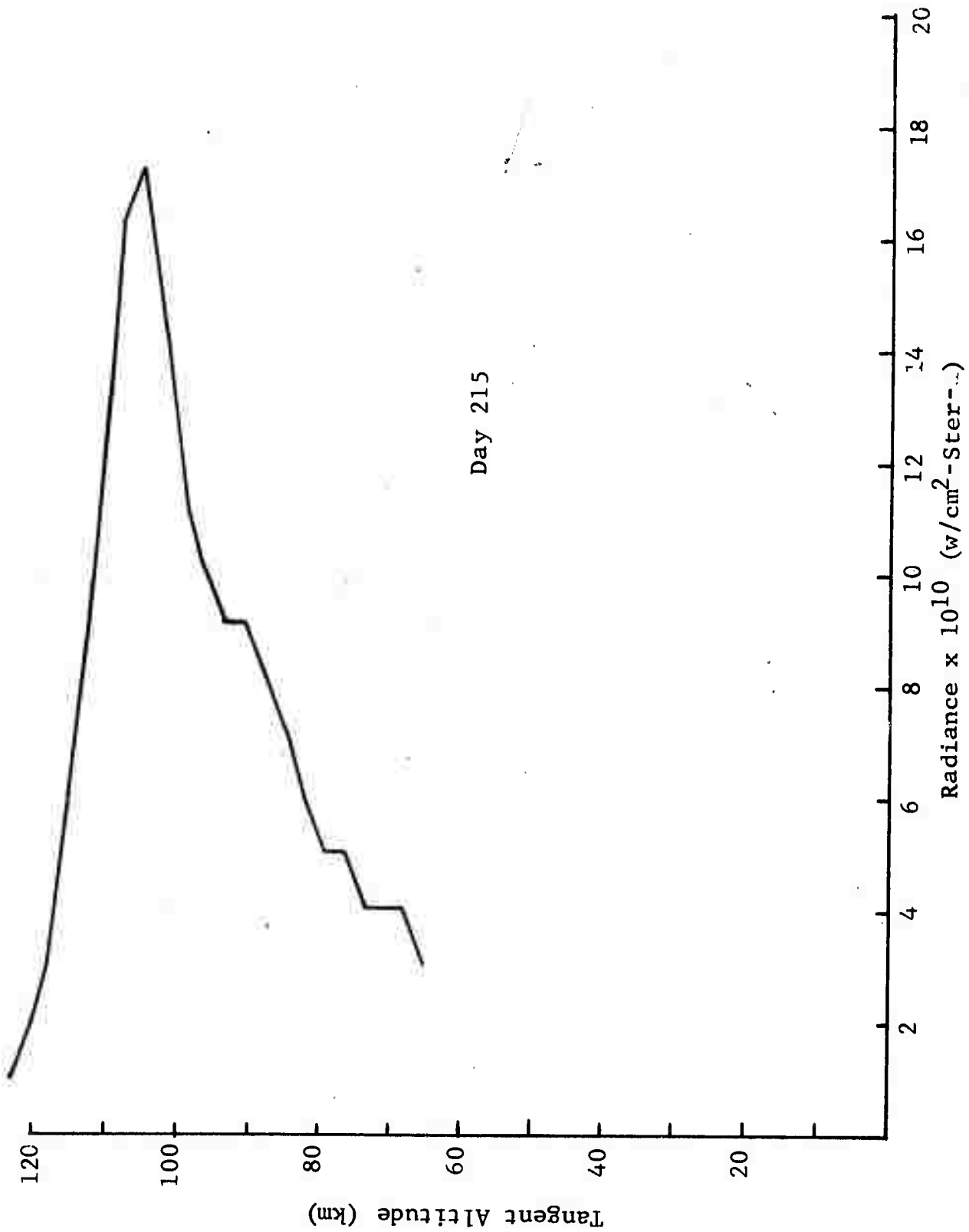


Fig. 19 Altitude Profile of 2380\AA Nightglow

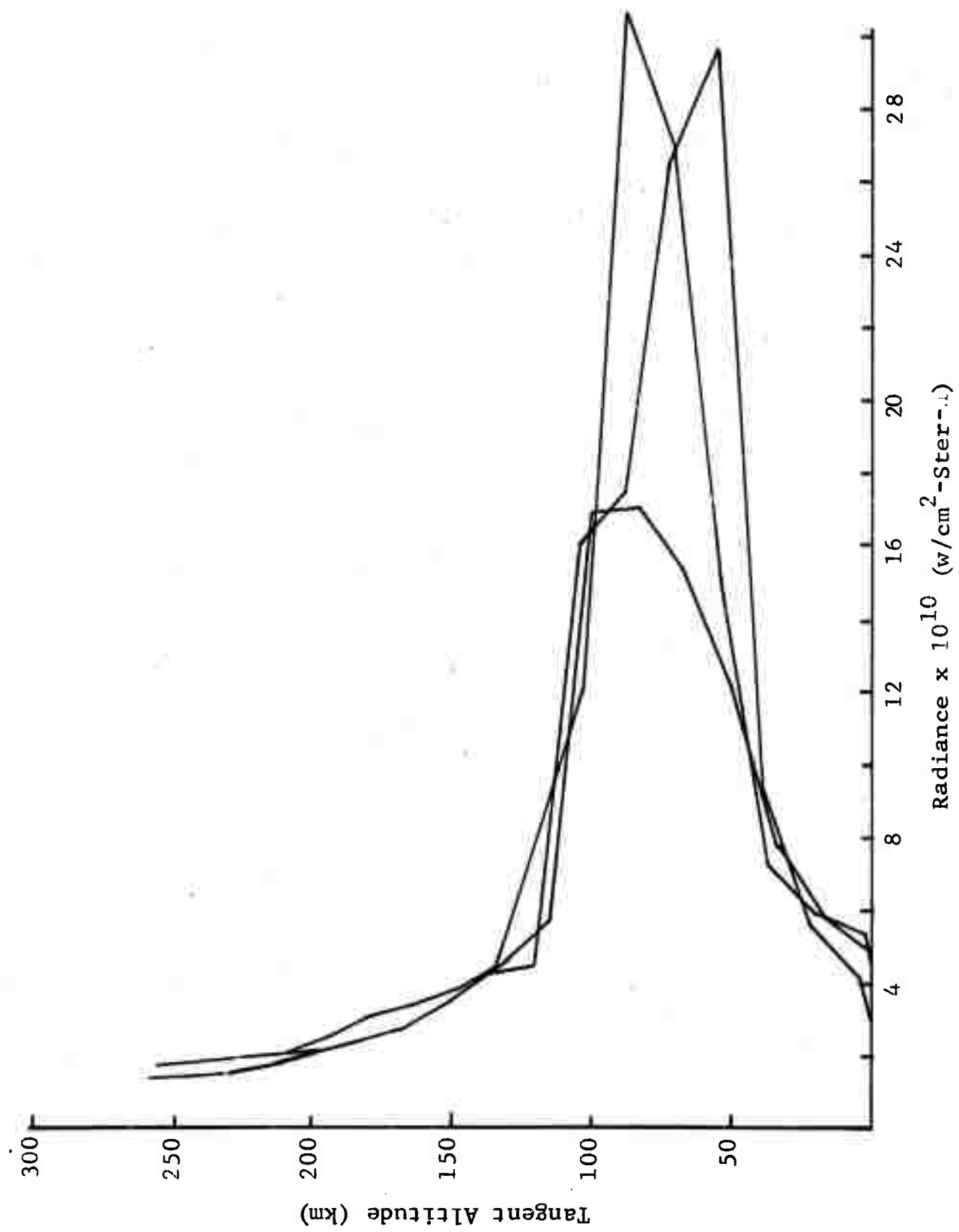


Fig. 20 Altitude Profile of the 2460\AA Nightglow

SUMMARY AND CONCLUSIONS

All earth background measurements made with the OAO A-2's Wisconsin Experiment Package have been analyzed in terms of viewing geometry, and have been converted to equivalent earth's radiance. This information has been summarized and placed on a computer tape, the printout of which is given in Table 5.

Samples of the measurements were analyzed every three minutes when observing the dark earth, every minute for sunlit observations, and every 10 seconds for measurements of the earth's limb. The GMT time of the measurements, the tangent altitude, the solar, viewing, and scattering angles, the OAO and viewing intersection longitude and latitude, as well as the reduced radiance for seven of the filter combinations, are given for each point analyzed.

An analysis of the reduced data has provided the following conclusions:

- 1) The dayglow in the 1920\AA spectral region is produced by the Rayleigh scattering of solar radiation. No significant radiation is produced above 100 kilometers.
- 2) In the $1300-1700\text{\AA}$ region, the measurements support the theory that the radiation is produced by photoelectron excitation of nitrogen (N_2). This radiation has a peak in the emission rate near 175 kilometers.
- 3) The nightglow below 1700\AA is quite low, less than $1.5 \times 10^{-8} \text{ w/cm}^2\text{-ster-}\mu$. There is some radiation produced by an unknown source, present in the 1920\AA region. This radiation has a peak intensity near 70 kilometers.
- 4) The prominent feature of the UV nightglow is the radiation between 2500 and 3000\AA that is thought to be the emissions from the Herzberg bands of molecular oxygen. This radiation shows a very sharp peak near 110 kilometers.

To complete the interpretation of these data, all measurements should be reduced into volume emission rates, and a detailed model of the radiation mechanisms should be developed. The reduction of

the nightglow measurements should be the simplest of these tasks. This involves inverting the limb measurements in a manner similar to that used by Robles and Hayes (Ref. 16). Reduction of the dayglow measurements is more complicated since the volume emission rates are dependent on the sun's position. The inversion is, therefore, not straightforward. A detailed model for the radiation mechanism, such as given by Eq. (13) for photoelectron excitation, is also required for a complete analysis of the measurements. Also needed are limb measurements at 1250, 1380, and 2380 \AA to complete the spectral picture of the ultraviolet earth background. Complete sets of measurements should be made at various times during the year to obtain seasonal variations in atmospheric emissions. Most observations made thus far with the OAO have been in the northern hemisphere. Therefore, additional measurements are required over various portions of the earth to obtain a global picture of the UV emissions. It appears that the best experiment for such measurements would be an imaging system with a large field of view and the comparable resolution of the WEP. This would provide significant information about local and global variations of the background.

REFERENCES

1. Barth, C. and Mackey, E., IEEE Trans. Geo. Elec., Vol. GE-7, No. 2, 1969, p. 114.
2. Barth, C. and Schaffner, S. J. Geophys. Res., Vol. 75, No. 22, 1970, p. 4299.
3. Chubb, T. and Hicks, G., J. Geophys. Res., Vol. 75, No. 7, 1970, p. 1290.
4. Meier, R. and Mange, P., Planet. Space Sci., Vol. 18, 1970, p. 803.
5. Prinz, D. and Meier, R., J. Geophys. Res., Vol. 76, No. 19, 1971, p. 4608.
6. Chamberlain, J., Physics of the Aurora and Airglow, 1961, Academic Press, New York.
7. Winter, W. and Chubb, T., J. Geophys. Res., Vol. 72, No. 21, 1967, p. 4405.
8. Fastie, W., Crosswhite, H., and Heath, D., J. Geophys. Res., Vol. 69, No. 19, 1964, p. 4129.
9. Green, A. and Barth, C., J. Geophys. Res., Vol. 72, No. 15, 1967, p. 3975.
10. Dalgarno, A., McElroy, M., and Stewart, A., J. Astron. Sci., Vol. 26, 1969, p. 753.
11. Barth, C., J. Geophys. Res., Vol. 69, No. 15, 1964, p. 3301.
12. Hinteregger, H., J. Geophys. Res., Vol. 66, 1961, p. 2367.
13. Ditchburn, R and Young, P., J. Atmos. Terr. Phys., Vol. 24, 1962, p. 127.
14. Hennes, J., J. Geophys. Res., Vol. 71, No. 3, 1966, p. 763.
15. Stecher, T., J. Geophys. Res., Vol. 70, No. 9, 1965, p. 2209.

16. Hays, P. and Roble, R., Report 08953-1-T, University of Michigan, 1967.
17. Elliott, D., Clark, M., and Hudson, R., Aerospace Report No. TR-1058 (3260-10), 1967.
18. Craig, R., The Upper Atmosphere, Academic Press, New York, 1965.
19. Green, A., The Middle Ultraviolet; Its Science and Technology, J. Wiley, New York, 1967.
20. Green, A. and Wyatt, P., Atomic and Space Physics, 1965.
21. Prinz, D. and Meier, R., Private Communication, 1971.